

Accepted Manuscript

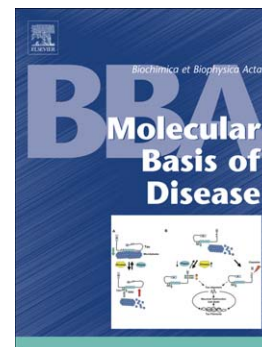
Activation of the endoplasmic reticulum stress response by the amyloid-beta 1-40 peptide in brain endothelial cells

Ana Catarina R.G. Fonseca, Elisabete Ferreiro, Catarina R. Oliveira, Sandra M. Cardoso, Cláudia F. Pereira

PII: S0925-4439(13)00272-X
DOI: doi: [10.1016/j.bbadis.2013.08.007](https://doi.org/10.1016/j.bbadis.2013.08.007)
Reference: BBADIS 63784

To appear in: *BBA - Molecular Basis of Disease*

Received date: 26 February 2013
Revised date: 28 July 2013
Accepted date: 20 August 2013



Please cite this article as: Ana Catarina R.G. Fonseca, Elisabete Ferreiro, Catarina R. Oliveira, Sandra M. Cardoso, Cláudia F. Pereira, Activation of the endoplasmic reticulum stress response by the amyloid-beta 1-40 peptide in brain endothelial cells, *BBA - Molecular Basis of Disease* (2013), doi: [10.1016/j.bbadis.2013.08.007](https://doi.org/10.1016/j.bbadis.2013.08.007)

This is a PDF file of an unedited manuscript that has been accepted for publication. As a service to our customers we are providing this early version of the manuscript. The manuscript will undergo copyediting, typesetting, and review of the resulting proof before it is published in its final form. Please note that during the production process errors may be discovered which could affect the content, and all legal disclaimers that apply to the journal pertain.

Activation of the endoplasmic reticulum stress response by the amyloid-beta 1-40 peptide in brain endothelial cells

Ana Catarina RG Fonseca^{ab}, Elisabete Ferreiro^a, Catarina R Oliveira^{a,c}, Sandra M Cardoso^{a,c}, and Cláudia F Pereira^{a,c}

^aCenter for Neuroscience and Cell Biology, University of Coimbra, Largo Marquês de Pombal, 3004-517 Coimbra, Portugal

^bDepartment of Life Sciences, Faculty of Sciences and Technology, University of Coimbra, Apartado 3046, 3001-401 Coimbra, Portugal

^cFaculty of Medicine, University of Coimbra, Rua Larga, 3004-504 Coimbra, Portugal

Corresponding author: Cláudia Maria Fragão Pereira, Center for Neuroscience and Cell Biology, University of Coimbra, Largo Marquês de Pombal, 3004-517 Coimbra, Portugal

Tel: +351239820190; Fax: +351239822776; E-mail: claudia.mf.pereira@gmail.com.

Abstract

Neurovascular dysfunction arising from endothelial cell damage is an early pathogenic event that contributes to the neurodegenerative process occurring in Alzheimer's disease (AD). Since the mechanisms underlying endothelial dysfunction are not fully elucidated, this study was aimed to explore the hypothesis that brain endothelial cell death is induced upon the sustained activation of the endoplasmic reticulum (ER) stress response by amyloid-beta ($A\beta$) peptide, which deposits in the cerebral vessels in many AD patients and transgenic mice. Incubation of rat brain endothelial cells (RBE4 cell line) with $A\beta_{1-40}$ increased the levels of several markers of ER stress-induced unfolded protein response (UPR), in a time-dependent manner, and affected the Ca^{2+} homeostasis due to the release of Ca^{2+} from this intracellular store. Finally, $A\beta_{1-40}$ was shown to activate both mitochondria-dependent and -independent apoptotic cell death pathways. Enhanced release of cytochrome c from mitochondria and activation of the downstream caspase-9 were observed in cells treated with $A\beta_{1-40}$ concomitantly with caspase-12 activation. Furthermore, $A\beta_{1-40}$ activated the apoptosis effectors' caspase-3 and promoted the translocation of apoptosis-inducing factor (AIF) to the nucleus demonstrating the involvement of caspase-dependent and -independent mechanisms during $A\beta$ -induced endothelial cell death. In conclusion, our data demonstrate that ER stress plays a significant role in $A\beta_{1-40}$ -induced apoptotic cell death in brain endothelial cells suggesting that ER stress-targeted therapeutic strategies might be useful in AD to counteract vascular defects and ultimately neurodegeneration.

Keywords

Alzheimer's disease; amyloid-beta peptide; endothelial cells; endoplasmic reticulum stress; calcium homeostasis; apoptosis

Abbreviations

AD, Alzheimer's disease; AIF, apoptosis-inducing factor; AM; acetoxymethyl ester; APP, amyloid precursor protein; ATF, activating transcription factor; $A\beta$, amyloid-beta; BBB, blood-brain barrier; bFGF, basic Fibroblast Growth Factor; CHOP, CAAT/enhancer binding protein homologous protein; DMSO, dimethyl

sulfoxide; ECF, Enhanced chemiFluorescence; ECs, endothelial cells; eIF2 α ; α subunit of eukaryotic translation initiation factor 2; ER, endoplasmic reticulum; GAPDH, glyceraldehyde-3-phosphate dehydrogenase; GRP78, glucose-regulated protein of 78 kDa; IRE1, inositol-requiring protein-1; JNK, c-jun N-terminal kinase; LDH, lactate dehydrogenase; LRP, low-density lipoprotein receptor-related protein; MTT, 3-(4,5-dimethylthiazol-2-yl)-2,5-diphenyltetrazolium bromide; NAD⁺, oxidized nicotinamide adenine dinucleotide; NADH, nicotinamide adenine dinucleotide; PARP1, poly(ADP-ribose) polymerase 1; PERK; protein kinase RNA-like ER kinase; PI, propidium iodide; PS, presenilinM; PVDF, Polyvinylidene difluoride; RAGE, receptor for advanced glycation end products; RBE4, rat brain endothelial cell line; RT, room temperature; Ry, ryanodine; RyR, ryanodine receptor; SDS-PAGE, SDS-polyacrylamide gel; SERCA, sarco/ER Ca²⁺ ATPase; TBP, TATA-binding protein; TBS-T, TBS-Tween; ThS, thioflavine S; TUNEL, terminal deoxynucleotidyl transferase dUTP nick-end labeling; UPR, unfolded protein response; WB, Western blot; XBP-1, X-box binding protein-1; $\Delta\psi_{mit}$, mitochondrial membrane potential.

1. Introduction

According to the 'Amyloid Cascade Hypothesis', the accumulation of amyloid-beta (A β) in brain parenchyma is responsible for the neurodegenerative process in Alzheimer's disease (AD) [1]. Furthermore, numerous studies support that neurovascular dysfunction contributes to neurodegeneration and cognitive decline and thus have a major role in AD pathogenesis (reviewed in [2]). First, vascular risk factors such as diabetes, obesity, hypercholesterolemia, hypertension, atherosclerosis, and stroke significantly increase the risk to develop AD [3, 4]. Second, combined evidences from neuroimaging and neuropathological studies show that signs of vascular pathology develop early in AD and occur before the disease becomes symptomatic [5, 6]. Third, deficient clearance of A β across the blood-brain barrier (BBB) has been described in the brain of AD patients [2]. Finally, A β deposition was found in the cerebral microvasculature of AD transgenic mice and in cerebrovessels in many AD patients and contributes to the age-dependent degeneration of cerebral vasculature and development of cerebral amyloid angiopathy, characterized by dysfunction of brain capillary endothelium [7, 8]. This dysfunction correlates with the toxic effects of A β on endothelial cells (ECs) and has

been extensively described in cultured cells, in isolated vessels as well as in whole animals [9-12]. A β induces irreversible morphological and functional changes of ECs resulting in suppression of their proliferative activity and reduced survival [13, 14]. In addition, A β -induced apoptosis was demonstrated in cultured cerebral ECs [9], but the underlying mechanisms have not been fully elucidated. It was reported that endoplasmic reticulum (ER) stress is a stimulus that initiates apoptotic cell death pathways in vascular ECs [15, 16], but its role in A β -induced endothelial dysfunction has not been addressed yet.

The ER is the principal organelle responsible for proper folding/processing of nascent proteins and Ca²⁺ homeostasis. Perturbed ER function leads to a state known as ER stress. To ameliorate this stress, mammalian cells possess a homeostatic set of protein signalling pathways and transcription factors termed the unfolded protein response (UPR). The UPR utilizes three types of ER-resident sensor proteins, inositol-requiring protein-1 (IRE1), protein kinase RNA-like ER kinase (PERK), and activating transcription factor 6 (ATF6), that are activated after the ER-resident chaperone glucose-regulated protein of 78kDa (GRP78, also known by immunoglobulin binding protein, BiP) dissociates from their ER luminal domains and initiate ER-to-nucleus signalling cascades to maintain the homeostasis [17, 18]. However, persistent and severe ER stress triggers apoptotic cascades resulting in cell death [19]. Upon dimerization and autophosphorylation, PERK inactivates the α subunit of eukaryotic translation initiation factor 2 (eIF2 α) by phosphorylation at Ser51, required for 80S ribosome assembly, thus inhibiting general protein translation through a decrease in the GTP-bound form of eIF2 α , but increasing the translation of the transcription factor ATF4. In the nucleus, ATF4 induces the transcription of several genes involved in controlling the UPR and growth arrest and DNA damage-inducible protein-34 (GADD34). GADD34 induces a negative feedback and dephosphorylates eIF2 α [20, 21]. IRE1 α removes a 26-base intron of mRNA of X-box binding protein-1 (XBP-1) inducing a more efficient translation and a more stable protein. The resulting XBP-1 protein with 54 kDa instead of 33 kDa comprises the original N-terminal DNA binding domain and a transactivation domain in the C-terminal and is a transcription factor that regulates genes involved in the ER-associated degradation pathway and increases the expression of several ER resident chaperones, such as GRP78 [22]. Upon dissociation from GRP78, ATF6 migrates to the Golgi apparatus where it is cleaved to release a transcription factor that upregulates

genes involved in amplification of folding capacity such as chaperones including GRP78 and also genes for protein disulfide isomerases, CAAT/enhancer binding protein homologous protein (CHOP, also termed GADD153), XBP-1 [21, 23], and genes involved in angiogenesis and autophagy [20]. During prolonged ER stress, apoptotic cell death is induced by the c-jun N-terminal kinase (JNK) pathway, by caspases, including the ER membrane-associated caspase-12 (in murine or the homologue caspase-4 in humans) or upregulation of the transcription of CHOP [19, 24]. CHOP functions to block cells transition from G1 to S phase during cell cycle progression and can directly activate GADD34 increasing oxidation reactions at the ER [25]. Furthermore, CHOP down-regulates Bcl-2 and induces the translocation of Bax to mitochondria and subsequent cytochrome c release and activation of the apoptosis-effector caspase-3 [26]. Besides, ER and mitochondria are physically close and in contact and communicate through Ca^{2+} signals [27]. In normal conditions, Ca^{2+} released from ER is taken up by mitochondria and increases ATP production. Nevertheless, an overload in Ca^{2+} uptake by mitochondria upon ER Ca^{2+} release promoted by apoptotic stimuli or ER stress could induce the release of cytochrome c and other caspase cofactors leading to apoptotic cell death [27]. In neurons, the mitochondrial uptake of Ca^{2+} released from ER is essential to activate the mitochondrial apoptotic cell death pathway under $\text{A}\beta_{1-40}$ -induced ER stress conditions [28].

Reports are available describing the engagement of ER stress in AD. In brain post-mortem samples from early AD patients, but not in non-demented subjects, ER stress markers have been detected in the temporal cortex and hippocampus [29]. Moreover, in transgenic mice modelling AD, increased brain levels of several ER stress markers have been described [30, 31]. The presenilins (PSs, components of the γ -secretase complex present in the ER membrane) function as low-conductance, passive ER Ca^{2+} leak channels and, consequently, familial AD-linked PSs mutations disturb ER Ca^{2+} homeostasis leading to increased susceptibility to activation of UPR and caspase-4-induced apoptosis [19, 32, 33]. Nonetheless, mutant PS1 reduces global ER function since it suppresses the activation of IRE1 α , ATF6, and PERK and, as a result, GRP78/BiP is downregulated in PS1 mutant AD patients [19]. GRP78/BiP is able to bind the amyloid precursor protein (APP) inhibiting $\text{A}\beta$ generation [34, 35]. Therefore, mutant PS1 may increase the generation of $\text{A}\beta$ by reducing the levels of GRP78/BiP available to bind APP. Moreover, aberrant splicing of

PS2, almost exclusively observed in the brains of sporadic AD patients, increases the production of A β and the vulnerability to ER stress [36] and, may thus be implicated in the pathogenesis of this form of the disease. Our previous *in vitro* results highlighted the role of ER stress in neuronal dysfunction triggered by A β [37, 38] but the impact of ER stress in A β -induced endothelial dysfunction has not been investigated yet. Therefore, the aim of this work was to analyze the molecular basis of cerebrovascular alterations in AD exploring the hypothesis that A β_{1-40} , which preferentially accumulates in brain vasculature [8, 39], damages microvascular brain ECs through induction of ER stress-mediated cell death pathways.

2. Experimental procedures

2.1. Materials

Indo-1 acetoxymethyl ester (Indo-1/AM), Alexa Fluor 488 goat anti-rabbit IgG conjugate, Fura-2 acetoxymethyl ester (Fura-2/AM), Tetramethylrhodamine methyl ester (TMRM), and Hoechst 33342 were obtained from Molecular Probes (Leiden, The Netherlands). The synthetic A β_{1-40} peptide was from Bachem (Bubendorf, Switzerland). Ionomycin, ProteoExtract® Subcellular Proteome Extraction Kit, and colorimetric substrates for caspase-3, -9 and -12 (Ac-DEVD-pNA, Ac-LEHD-pNA, and Ac-LEVD-pNA, respectively) were purchased from Calbiochem (Darmstadt, Germany). Polyvinylidene difluoride (PVDF) membrane, goat alkaline phosphatase-linked anti-rabbit and anti-mouse secondary antibodies, and the Enhanced chemiFluorescence (ECF) reagent were acquired from Amersham Pharmacia Biotech (Buckinghamshire, UK). Mouse monoclonal antibody against glyceraldehyde-3-phosphate dehydrogenase (GAPDH) was from Chemicon International Inc. (Temecula, CA, USA). The Glycergel Mounting Medium was purchased from DakoCytomation Inc. (Carpinteria, CA, USA). Bio-Rad protein dye assay reagent, acrylamide, and the prestained Precision Plus Protein All Blue Standard were purchased from Bio-Rad (Hercules, CA, USA). The *In Situ* Cell Death Detection Kit, Fluorescein (with terminal deoxynucleotidyl transferase dUTP nick-end labeling, TUNEL), and collagen were obtained from Roche Applied Science (Mannheim, Germany). Trypsin EDTA solution, thioflavin S (ThS), 3-(4,5-dimethylthiazol-2-yl)-2,5-diphenyl tetrazolium bromide (MTT), anti- α -tubulin mouse monoclonal antibody, protease inhibitors (leupeptin, pepstatin A, chymostatin, and aprotinin),

thapsigargin, recombinant human basic Fibroblast Growth Factor (bFGF), oligomycin, carbonyl cyanide 4-(trifluoromethoxy)phenylhydrazone (FCCP), dantrolene sodium, and mouse monoclonal antibody reactive against ATF4 were obtained from Sigma Chemical Co. (St. Louis, MO, USA). Rabbit polyclonal antibodies reactive against XBP1 and mouse monoclonal antibody reactive against TATA-binding protein (TBP) were acquired from Abcam plc (Cambridge, UK). Mouse monoclonal antibodies reactive against GRP78 and cytochrome c, and rabbit polyclonal antibody reactive against caspase-12 were from BD Biosciences (Heidelberg, Germany). Mouse monoclonal antibodies reactive against CHOP/GADD153 or apoptosis-inducing factor (AIF), and rabbit polyclonal antibodies reactive against ATF6 α or Tom20 were obtained from Santa Cruz Biotechnology Inc. (Santa Cruz, CA, USA). Rabbit polyclonal antibodies reactive against Bax or cleaved poly(ADP-ribose) polymerase 1 (PARP1) (Asp214), and rabbit monoclonal antibody against Bcl-2 were acquired from Cell Signaling Technology, Inc. (Danvers, MA, USA). Mem-Alpha medium with Glutamax-1, Nut Mix F-10 W/GLUTAMAX-1, and geneticin were acquired from Invitrogen Life Science (Paisley, UK).

2.2. Culture of rat brain endothelial cell line RBE4 and treatments

The rat brain endothelial cell line RBE4 was provided by Dr. Jon Holy (University of Minnesota, Duluth, USA). RBE4 is a continuous, immortalized cell line that retains a stable phenotype reminiscent of BBB endothelium in vitro [40]. Cells at passages 10-35 were grown on 75 cm² tissue culture flasks coated with 4.15 $\mu\text{g}/\text{cm}^2$ collagen in MEM-Alpha medium with Glutamax-1 and Nut Mix F-10 W/GLUTAMAX-1 (1:1 vol/vol), supplemented with 1 ng/ml bFGF and 0.3 mg/ml geneticin. Cells were maintained at 37°C in a humidified atmosphere of 5% CO₂/95% air.

RBE4 cells were plated on collagen-coated (4.15 $\mu\text{g}/\text{cm}^2$) multiwell plates at a density of approximately 22,000 cells/cm² and were then treated with 0.1 or 2.5 μM A β_{1-40} during 3-24 hr. Thereafter, cell viability, protein levels of ER stress markers as well as of apoptosis, levels of cytosolic Ca²⁺, mitochondrial membrane potential ($\Delta\psi_{\text{mit}}$), and also caspases-3, -9 and -12-like activities were measured. Alternatively, RBE4 cells plated in coverslips coated with poly-L-lysine (0.1 mg/ml) and then collagen (4.15 $\mu\text{g}/\text{cm}^2$) were treated with

2.5 μM $\text{A}\beta_{1-40}$ for 3, 6, 12 or 24 hr and after that fibrillar content, ATF6 nuclear localization, necrotic/apoptotic cell death markers, and ER Ca^{2+} content were analyzed.

Synthetic $\text{A}\beta_{1-40}$ -HCl was dissolved in sterile water at a concentration of 6 mg/ml and then diluted to 1 mg/ml (231 μM) in PBS and stored at -20°C until use.

2.3. Detection of $\text{A}\beta$ fibrils in cell culture

The presence of β -sheet fibrils has been assessed by ThS staining in RBE4 cells treated with 2.5 μM “fresh” $\text{A}\beta_{1-40}$ during 3 hr. In brief, control and treated cells were washed with PBS buffer (pH 7.4) and were fixed with 4% paraformaldehyde for 15 min at RT. The cells were permeabilized with 0.2% Triton X-100 in PBS buffer (pH 7.4), for 2 min, at RT and were then incubated with a 1% ThS solution for 20 min in the dark. Cells were subsequently washed with PBS buffer (pH 7.4), with a 70% ethanol solution (quick wash) and finally with PBS. Then, coverslips mounted in DakoCytomation Fluorescent mounting solution on a microscope slide for the visualization in a fluorescence microscope (Zeiss axioskop2, Zeiss, Jena, Germany).

2.4. Analysis of cell viability by the MTT assay

Cell viability was evaluated using the MTT assay, which measures the ability of metabolic active cells to form formazan through cleavage of the tetrazolium ring of MTT [41]. Briefly, cells were washed in normal sodium medium (in mM: 132 NaCl, 4 KCl, 1.2 Na_2HPO_4 , 1.4 MgCl_2 , 6 glucose, 10 HEPES, and 1 CaCl_2 , pH 7.4) and incubated with 0.5 mg/ml MTT for 2 hr at 37°C . The blue formazan crystals formed were dissolved in an equal volume of 0.04 M HCl in isopropanol and quantified spectrophotometrically by measuring the absorbance at 570 nm using a microplate reader (SpectraMax Plus 384, Molecular Devices, California, USA). Results were expressed as the percentage of the absorbance determined in control cells.

2.5. Analysis of plasma membrane integrity by the lactate dehydrogenase (LDH) assay

The integrity of the plasma membrane was evaluated by determining the release of the cytoplasmic enzyme LDH as previously described [42]. The activity of intracellular and released LDH was determined

spectrophotometrically (Pharma Spec, UV-1700, UV-Visible spectrophotometer, Shimadzu), by following the rate of conversion of reduced nicotinamide adenine dinucleotide (NADH) to oxidized nicotinamide adenine dinucleotide (NAD⁺) at 340 nm. After cell treatment, the medium was collected (extracellular LDH) and the cells were lysed in 10 mM HEPES (pH 7.4) plus 0.01% (v/v) Triton X-100 (intracellular LDH) followed by 3 cycles of freezing (-80°C) and thawing. In both intra and extracellular aliquots, cell debris were removed by centrifugation at 20,800 g for 10 min. LDH release into the extracellular medium was calculated as the percentage of total LDH activity (extracellular + intracellular LDH), and then expressed relatively to the control.

2.6. Quantification of apoptotic and necrotic cells by the TUNEL assay and using Hoechst

33342/propidium iodide staining

Apoptotic cell death was analyzed by the TUNEL assay [28], performed using an *In Situ* Cell Death Detection Kit, according to the manufacturer's directions. ECs cultured on glass coverslips were washed in PBS buffer (pH 7.4) and fixed with 4% (w/v) paraformaldehyde for 30 min at room temperature (RT). Then, slides were rinsed twice in PBS buffer and immersed in 0.1% (v/v) Triton X-100 supplemented with 0.1% (w/v) sodium citrate in iced PBS, for 2 min, to permeabilize the cells. Coverslips were rinsed again 3 times with PBS and incubated with TUNEL mixture for 1 hr at 37°C, in the dark. Finally, coverslips were rinsed 3 times with PBS and mounted with Glycergel Mounting Medium onto a microscope slide for visualization in a fluorescence microscope (Zeiss axioskop2, Zeiss, Jena, Germany) with a 40x objective. DNase-treated cells were used as a positive control.

The number of apoptotic and necrotic cells was analyzed by nuclear morphology criteria using Hoechst 33342 (which is able to cross cell membranes and binds chromatin) and propidium iodide (PI, which only cross damaged membranes and binds chromatin) staining in live cells. After treatment in coverslips, ECs were washed two times with PBS at 37°C, incubated with 15 µg/ml Hoechst 33342 and 3 µg/ml PI in PBS for 5 min in the dark, washed again two times with PBS and mounted with PBS at 37°C on a microscope slide and observed in a fluorescence microscope (Zeiss axioskop2, Zeiss, Jena, Germany) using a 40x objective.

Viable cells display a normal nuclear size without PI staining. The cells with normal nuclear size with PI staining were scored as necrotic cells. Scored apoptotic ECs include cells that display pyknotic nuclei with condensed or fragmented chromatin with or without PI staining (primary and secondary apoptotic cells). All experiments were performed three times in duplicate, and a minimum of 150 cells were scored for each coverslip. The number of apoptotic and necrotic cells were expressed as the percentage (%) of the total number of cells in all microscope fields for each coverslip.

2.7. Western blot analysis of ER stress and apoptotic markers

Proteins levels of ER stress markers were evaluated by immunoblotting using cellular extracts obtained from treated or untreated ECs. First, cells were washed 2 times with PBS (pH 7.4) and scraped in ice cold lysis buffer (in mM): 25 HEPES-Na, 2 MgCl₂, 1 EDTA, 1 EGTA, supplemented with 0.1 mM PMSF, 2 mM DTT, and 1:1000 of a protease inhibitor cocktail (1 µg/ml leupeptin, pepstatin A, chymostatin, and antipain). The cellular extracts were then rapidly frozen in liquid N₂ and thawed, centrifuged for 1 min at 106 g at 4°C and the supernatant was collected. Apoptotic markers protein levels were also evaluated by immunoblotting using cytosolic, nuclear or mitochondrial fractions from treated or untreated ECs obtained with the ProteoExtract® Subcellular Proteome Extraction Kit according to the manufacture's instruction. The protein content was measured using the Bio-Rad protein dye assay reagent.

Total cellular extracts containing 15 µg protein, or cytosolic, nuclear and mitochondrial fractions containing 30 µg protein, were separated by electrophoresis on 10% (w/v) SDS-polyacrylamide gel (SDS-PAGE) after denaturation at 95°C for 5 min in sample buffer (in mM): 100 Tris, 100 DTT, 4% (v/v) SDS, 0.2% (w/v) bromophenol blue and 20% (v/v) glycerol. To facilitate the identification of proteins of interest, the prestained Precision Plus Protein All Blue Standards was used. Proteins were then transferred to PVDF membranes, which were further blocked for 1 hr at RT with 5% (w/v) BSA in Tris-buffered saline (150 mM NaCl, 50 mM Tris, pH 7.6) with 0.1% (w/v) Tween 20 (TBS-T). The membranes were next incubated overnight at 4°C with a primary mouse monoclonal antibody against GRP78 (1:1,000 dilution in TBS-T), CHOP/GADD153 (1:500 dilution in TBS-T), ATF4 (1:250 dilution in TBS-T), cytochrome c (1:500 dilution in TBS-T) or AIF (1:1000

dilution in TBS-T) or with a primary rabbit antibody against pro-caspase-12 (1:1,000 dilution in TBS-T), ATF6 α (1:1,000 dilution in TBS-T), XBP1 (1:1,000 dilution in TBS-T), Bcl-2 (1:1,000 dilution in TBS-T) or Bax (1:1,000 dilution in TBS-T). Control of protein loading was performed using a primary mouse against GAPDH antibody (1:1,000 dilution in TBS-T) or a primary mouse anti- α -tubulin antibody (1:20,000 dilution in TBS-T) for total cellular or cytosolic extracts, a primary rabbit anti-Tom20 antibody (1:500 dilution in TBS-T) for mitochondrial extracts, and a primary mouse against TBP antibody (1:2,000 dilution in TBS-T) for nuclear extracts. After washing, membranes were incubated for 1 hr at RT with an alkaline phosphatase conjugated secondary anti-mouse or anti-rabbit antibody (1:20,000 dilution in TBS-T). Bands of immunoreactive proteins were visualized after membrane incubation with ECF reagent during approximately 5 min, on a Versa Doc 3000 Imaging System (Bio-Rad, Hercules, CA, USA) and densities of protein bands were calculated using the WCIF ImageJ program (Wayne Rasband, Research Services Branch, National Institute of Mental Health, Bethesda, Maryland, USA). The ratios between pro-caspase-12, caspase-12, or AIF and GAPDH, the ratios between GRP78, ATF6 α , GADD153, XBP1, or ATF4 and α -tubulin, the ratios cytochrome c in mitochondria/total (cytochrome c in mitochondria plus cytochrome c in the cytosol), or cytochrome c in the cytosol/total and the ratios Bax/Bcl-2 in mitochondria or Bax/Bcl-2 in the cytosol were calculated and results were normalized to control values.

2.8. Evaluation of ATF6 activation or PARP1 cleavage by immunocytochemistry

In order to analyze the translocation of ATF6 to the nucleus or the cleavage of PARP1 by caspases, treated or untreated ECs grown in glass coverslips were rinsed two times with PBS (pH 7.4) and then fixed with 4% (w/v) paraformaldehyde at RT for 30 min. Cells were then washed two times with PBS. Coverslip-plated ECs were permeabilized with 0.2% (v/v) Triton X-100 for 2 min and were then incubated for 30 min at RT in blocking solution containing 3% (w/v) BSA in PBS to prevent non-specific binding. Subsequently, cells were incubated during 1 hr at 4°C with a primary rabbit anti-ATF6 α antibody or against the large fragment resulting from caspases cleavage of rat PARP1 (1:200 dilution in blocking solution). Thereafter, coverslips were rinsed in PBS and incubated for 1 hr at RT with the secondary antibody anti-rabbit IgG labelled with Alexa Fluor 488

(1:200 dilution) diluted in PBS with 1% (w/v) BSA. Following additional rinses in PBS, cells were stained in the dark for 5 min, at RT, with 15 µg/ml Hoechst 33342 prepared in PBS. Finally, the preparations were mounted using Glycergel Mounting Medium. Images were collected using a Zeiss LSM 510 Meta confocal microscope (Carl Zeiss, New York, USA) with a 63x objective or in a fluorescence microscope (Zeiss axioskop2, Zeiss, Jena, Germany) with a 40x objective. All experiments were performed three times in duplicate, and a minimum of 100 cells were scored for each coverslip. For ATF6α nuclear translocation analysis, the fluorescence and the area of cell nucleus were quantified using the WCIF ImageJ program (Wayne Rasband, Research Services Branch, National Institute of Mental Health, Bethesda, Maryland, USA) and the ratio fluorescence/area calculated.

2.9. Analysis of ER calcium content by single cell imaging with Fura-2/AM

The content of Ca²⁺ in the ER was measured by single cell Ca²⁺ imaging using the fluorescent probe Fura-2/AM, according to the method described by Ferreiro and colleagues [28]. Treated and untreated cells, plated in glass coverslips, were washed 2 times in sodium medium without Na₂HPO₄ (in mM: 132 NaCl, 4 KCl, 1 CaCl₂, 1.4 MgCl₂, 6 glucose, 10 HEPES-Na, pH 7.4) and supplemented with 10 mM NaHCO₃, 0.05 mM EGTA, and 0.1% (w/v) fatty acid-free BSA, pH 7.4. Then, cells were loaded with 5 µM Fura-2/AM in the same medium supplemented with 0.2% (w/v) pluronic acid for 40 min, at 37°C in the dark. Afterwards, cells were washed 3 times in Ca²⁺-free Krebs medium and the coverslips were assembled to perfusion chamber, in the same Ca²⁺-free medium, in an inverted fluorescence microscope (Axiovert 200, Zeiss, Jena, Germany). Cells were alternatively excited at 340 and 380 nm using a Lambda DG4 apparatus (Sutter Instruments Company, Novaco, CA, USA), and emitted fluorescence at 510 nm was collected with a 40x objective and was driven to a coll SNAP digital camera (Roper Scientific, Trenton, NJ, USA). After a baseline was established, cells were stimulated with thapsigargin (2.5 µM), to empty ER Ca²⁺ stores. Acquired values were processed using the MetaFluor software (Universal Imaging Corporation, Buckinghamshire, UK). The increase in 340/380 nm ratio is proportional to ER Ca²⁺ content and the absence of external Ca²⁺ guarantees that the increase in the Fura-2 fluorescence ratio is due solely to the release of Ca²⁺ from the ER. The peak amplitude of Fura-2

fluorescence (ratio at 340/380 nm) was used to evaluate ER Ca^{2+} content that was normalized to control values.

2.10. Measurement of cytosolic calcium concentration with Indo-1/AM

The cytosolic Ca^{2+} concentration was measured in RBE4 cells cultured on 24-well plates. Cells were incubated in the dark with 3 μM Indo-1/AM in sodium medium without Na_2HPO_4 for 45 min at 37°C, and were further incubated for 15 min in the absence of Indo-1/AM to ensure a complete hydrolysis of the acetoxymethyl ester. Subsequently, Indo-1 fluorescence was measured in a microplate reader (SpectraMax Gemini EM fluorocytometer, Molecular Devices, California, USA) with excitation at 350 nm and emission at 410 nm. The free cytosolic Ca^{2+} concentration was calculated using the F_{max} and AF (Autofluorescence) values determined after the addition of ionomycin (3 μM) and MnCl_2 (3 mM), respectively [43] and the results were expressed relatively to the control.

2.11. Mitochondrial membrane potential measurements

The $\Delta\psi_{\text{mit}}$ was measured using the fluorescent dye TMRM. This cationic indicator is accumulated preferentially into energized mitochondria driven by the membrane potential. In the final of the treatments, RBE4 cells were washed with PBS and incubated with 300 nM TMRM in sodium medium for 1 hr at 37°C in the dark. Then, the medium was replaced by sodium medium at 37°C and the fluorescence was measured in a microplate reader (SpectraMax Gemini EM fluorocytometer, Molecular Devices, California, USA) with excitation at 540 nm and emission at 590 nm (F). 1 μM FCCP and 2 $\mu\text{g/ml}$ oligomycin were added and the fluorescence measured again (F0). The differences between F and F0 were calculated and the results were expressed relatively to untreated cells.

2.12. Analysis of caspase-3, -9, and -12-like activity

The activation of caspases-3, -9, and -12 was investigated in extracts from control and treated RBE4 cells. After treatments, ECs were washed two times with PBS at 4°C and scraped in reaction buffer: 25 mM

HEPES-Na, 10% (w/v) sucrose, 10 mM DTT, and 0.1% (w/v) CHAPS (pH 7.4). The cellular extract was rapidly frozen and thawed three times in liquid N₂, and then centrifuged for 10 min at 20,800 g at 4°C. The supernatant was collected and assayed for protein content using the Bio-Rad protein dye assay reagent. Aliquots of cellular extracts containing 30 µg of protein were reacted with 0.1 mM Ac-DEVD-pNA (chromogenic substrate for caspase-3), Ac-LEHD-pNA (chromogenic substrate for caspase-9) or Ac-LEVD-pNA (chromogenic substrate for caspase-12), in reaction buffer for 2 hr at 37°C. Caspase-3, -9, and -12-like activity was determined by measuring substrate cleavage at 405 nm in a microplate reader (SpectraMax Plus 384) and results were expressed relatively to the control.

2.13. Data analysis

Data were expressed as means ± SEM of measurements performed in duplicate, from at least three independent experiments. Statistical significance analysis was determined using one-way ANOVA followed by Dunnett's post hoc tests or using Student's *t*-test in the GraphPad Prism Software (San Diego, CA, USA). The differences were considered significant for P values < 0.05.

3. Results

3.1. Aβ₁₋₄₀ peptide decreases brain endothelial cell survival and activates apoptotic cell death

Previously, we have shown that the addition of Aβ₄₀₋₁ to cell culture medium do not significantly affect cell's morphology and survival [37, 44], demonstrating the specificity of the amino acids sequence of Aβ₁₋₄₀. Here, incubation of RBE4 cells for 3-24 hr with 0.1 or 2.5 µM Aβ₁₋₄₀, which forms small aggregates in culture (Fig. 1A), decreased cell survival, as evaluated by the MTT assay, in a dose- and time-dependent manner (Fig. 1B). A statistical significant decrease in the ability to reduce MTT, and thus in cell viability, was observed when RBE4 cells were exposed to 0.1 µM Aβ₁₋₄₀ for 12 or 24 hr or to 2.5 µM Aβ₁₋₄₀ for 3 or more hours. Accordingly with these results, the Aβ₁₋₄₀ concentration of 2.5 µM was used in subsequent studies. Aβ₁₋₄₀ was shown to preserve the integrity of the plasma membrane since no significant release of LDH occurred after 6 or 24 hr (Fig. 1C), suggesting that necrosis doesn't contribute to Aβ-induced cell death in brain ECs. These

results were corroborated with Hoechst 33342/PI showing that the number of necrotic cells was not affected by A β ₁₋₄₀ treatment (Fig. 1D and E). Moreover, in RBE4 cells treated with 2.5 μ M A β ₁₋₄₀ during 24 hr, a significant increase in the number of apoptotic cells, as determined using Hoechst 33342/PI staining (Fig. 1D and E) and the TUNEL assay (Fig. 1F and G). Taken together, these results show that A β ₁₋₄₀ is toxic to brain ECs compromising cell survival and leading to the activation of an apoptotic cell death pathway.

3.2. A β ₁₋₄₀ induces ER stress in brain endothelial cells

The levels of several ER stress markers were determined in A β ₁₋₄₀-treated brain ECs by Western Blot (WB). Significant increases in proteins levels of ATF4 (Fig. 2A and B) (activated downstream of the PERK ER stress sensor), unspliced XBP1 (Fig. 2A and C) (the transcription of XBP-1 gene increases upon UPR activation), spliced XBP1 (Fig. 2A and D) (downstream of the IRE1 α ER stress sensor), active ATF6 α (Fig. 2A and E) (the 55 kDa fragment that results from ATF6 α cleavage within the Golgi apparatus), and the ER chaperone GRP78/BiP (Fig. 2A and F) were observed in RBE4 cells treated with A β ₁₋₄₀ for 3, 6, or 12 hr, but not 24 hr. The subcellular localization of ATF6 α was also followed by immunocytochemistry and a significant increase in ATF6 α staining was observed in cells treated with A β ₁₋₄₀ for 6 hr, especially in the nucleus, comparatively to that detected in control cells in the absence of A β ₁₋₄₀ treatment (Fig. 2G and H) supporting the nuclear translocation of cleaved ATF6 α under these conditions. These results demonstrate that ER stress is activated in ECs exposed to toxic A β ₁₋₄₀ concentrations.

3.3. ER and cytosolic calcium homeostasis is impaired by A β ₁₋₄₀ in brain endothelial cells

The levels of Ca²⁺ in the ER and in the cytosol were analyzed in ECs treated with 2.5 μ M A β ₁₋₄₀ for 3 or 24 hr and for 3, 6, 12, or 24 hr, respectively. Under these conditions, the ER Ca²⁺ content was shown to be significantly depleted in RBE4 cells after A β ₁₋₄₀ treatment, as analyzed by single cell Ca²⁺ imaging with Fura-2/AM (Fig. 3A and B). Moreover, a significant rise in cytosolic Ca²⁺ levels measured with Indo-1/AM was observed in A β ₁₋₄₀-treated cells (Fig. 3C). These results suggest that A β ₁₋₄₀ impairs ER Ca²⁺ homeostasis leading to the early release of Ca²⁺ from ER subsequently increasing cytosolic Ca²⁺ levels. Changes in ER

Ca²⁺ content are correlated with activation of ER stress sensors (Fig. 2). In addition, impairment of Ca²⁺ homeostasis precedes activation of apoptotic cell death (Fig. 1D-G).

3.4. Activation of the ER stress-mediated apoptotic pathway in A β ₁₋₄₀-treated brain endothelial cells

The levels of CHOP/GADD153, a pro-apoptotic transcription factor that is activated under ER stress conditions, were shown to be affected in RBE4 cells by A β ₁₋₄₀ in a time-dependent manner with a maximal increase observed at 3 and 6 hr of treatment (Fig. 4). Cytochrome c, Bax and Bcl-2 protein levels were also analyzed in cytosolic and mitochondrial sub-cellular fractions by WB and $\Delta\psi$ _{mit} after 3, 6, 12, or 24 hr of incubation with A β ₁₋₄₀ (Fig. 5). The ratio between Bax and Bcl-2 protein levels in mitochondria was significantly augmented with a maximal increase at 12 hr of treatment with A β ₁₋₄₀ (Fig. 5B). Concomitantly, this ratio decreased in the cytosol but statistical significance was only observed at 3 hr (Fig. 5C). Cytochrome c levels were significantly decreased in mitochondria (Fig. 5D) and increased in cytosol (Fig. 5E) with a maximum release from mitochondria determined after 12 hr of treatment with A β ₁₋₄₀. In addition, $\Delta\psi$ _{mit} decreased upon A β ₁₋₄₀ treatment with a minimum at 12 hr (Fig.5F) that was reverted by dantrolene (Fig. 5G). These results suggest that activation of CHOP/GADD153 under A β ₁₋₄₀-induced ER stress conditions promotes the translocation of Bax from the cytosol to the mitochondria, decreasing $\Delta\psi$ _{mit} and leading to cytochrome c release.

The activation of the ER resident caspase-12 was by WB. After exposure of RBE4 cells to A β ₁₋₄₀ during 3, 6, 12 or 24 hr, the levels of pro-caspase-12 were not significantly altered (Fig. 6A and B) but the levels of the active form caspase-12 increased until 12 hr of A β ₁₋₄₀ treatment returning to control values at 24 hr (Fig.6A and C). Furthermore, caspase-12-like activity was shown to be increased in A β ₁₋₄₀-treated cells after 6 and 12 hr incubation, but not at 24 hr (Fig. 6D). Similarly, a significant increase in caspase-like activities of caspase-9 (Fig. 6E) and caspase-3 (Fig. 6F) was determined 6 and 12 hr after A β ₁₋₄₀ exposure, but not at 24 hr. The cleavage of PARP1 by caspases, namely caspase-3, after incubation of RBE4 cells with 2.5 μ M A β ₁₋₄₀ during 12 or 24 hr was evaluated by immunocytochemistry using a specific antibody, which recognizes the large fragment with 89 kDa of PARP1 resulting from caspase cleavage at Asp214, and Hoechst 33342 to label

nuclei . An increase in cleaved PARP1 was observed in A β ₁₋₄₀-treated cells both after 12 and 24 hr incubation (Fig. 6G). Together, these results demonstrate that A β -induced ER stress leads to apoptotic cell death in ECs through mitochondria-independent pathways, mediated by caspase-12 activation, but also through mitochondria-dependent pathways that rely on the release of mitochondrial cytochrome c upon Bax translocation to mitochondria and subsequent activation of caspases-9 and -3 finally leading to cleavage of apoptosis substrates and cell death.

3.5. A β ₁₋₄₀-treatment induces the translocation of AIF to the nucleus

The release of AIF from mitochondria and subsequent translocation to the nucleus was evaluated by WB in mitochondrial and nuclear extracts obtained from control and A β ₁₋₄₀-treated RBE4 cells for 3 to 24 hr. The content of AIF in the cytosol was very low (Fig. 7A) suggesting that AIF released from mitochondria was rapidly degraded or translocated to the nucleus. After 24 hr of A β ₁₋₄₀ treatment, a slight decrease in mitochondrial AIF content (Fig. 7A and B) and a significant increase in AIF levels in the nucleus (Fig. 7A and C) were observed. These findings support that A β ₁₋₄₀-induced Bax translocation to the mitochondria also activates AIF-mediated caspase-independent cell death pathways.

4. Discussion

The results here presented using brain ECs treated with A β ₁₋₄₀ highlight the role of the ER stress-mediated apoptotic cell death pathway in vascular alterations that occur in AD brain. This hypothesis is supported by our findings demonstrating that A β ₁₋₄₀: i) compromises EC survival; ii) induces ER stress, increasing the levels of several mediators of UPR signalling pathways; iii) induces loss of ER Ca²⁺ homeostasis concomitantly increasing cytosolic Ca²⁺ levels; iv) upregulates the ER stress-associated pro-apoptotic transcription factor CHOP/GADD153; v) activates a mitochondria-independent cell death pathway associated with activation of the ER resident caspase-12; vi) triggers the early translocation of Bax to mitochondria leading to cytochrome c release and subsequent caspase-9 and caspase-3 activation (caspase-dependent

pathway) and also to the release of AIF from mitochondria and translocation to the nucleus (caspase-independent pathway).

AD patients frequently have deposits of A β in cerebral arteries, veins and capillaries possibly due to reduced trans-endothelial clearance of A β [7]. Previous studies demonstrate that A β could deregulate ECs causing morphological and functional alterations and inducing apoptosis [9, 13, 14]. However, the mechanisms responsible for A β -induced apoptotic cell death in these cells have not been fully elucidated. In this study, we demonstrated that A β_{1-40} affects the survival of brain ECs in a dose- and time-dependent manner using the RBE4 cell line. Furthermore, we were able to show that toxic concentrations of A β_{1-40} increase the percentage of apoptotic cells, in the absence of significant alterations in the number of necrotic cells.

We previously demonstrated that A β induces neuronal apoptosis through ER stress activation [37, 38]. In ECs, ER stress and consequent activation of UPR has been reported to be triggered by several stimuli [45-47]. Some metabolic diseases associated with vascular abnormalities, such as obesity and type 2 diabetes, are risk factors for AD [48] and are known to affect A β production [49]. Moreover, several studies indicate that ER stress contributes to the pathogenesis of obesity and diabetes [50]. A β_{1-40} inhibits human brain vascular ECs proliferation [14] and induces apoptosis [51]. However, the role of A β in the ER stress response in brain ECs is unknown. To demonstrate the effect of A β in the ER stress response in these cells, the levels of ATF4, spliced XBP-1, and cleaved ATF6 α , which occur downstream of the activation of the ER stress sensors PERK, IRE1, and ATF6, respectively, and also of GRP78, a molecular chaperone, and unspliced XBP-1 that are an ER stress target genes [17], were analyzed after A β_{1-40} treatment. A significant increase in the levels of these ER stress markers was detected in A β_{1-40} -treated RBE4 cells clearly indicating that A β_{1-40} activates the ER stress-associated UPR signalling pathways in brain ECs.

One of the functions of vascular ECs from the BBB is to remove A β from the brain. The accumulation of proteins inside the ER, which activates the UPR and consequently inhibits protein translation, decreases the traffic of proteins in the secretory pathway. Consequently, the levels of A β transporters at the plasma membrane can decrease leading to A β accumulation in brain. Accordingly, the ratio between A β efflux and influx in AD patients' brain is decreased compared to healthy subjects showing that A β clearance from the

brain is compromised in the disease [52]. Moreover, ER stress was demonstrated to increase A β production and subsequent accumulation [53]. The accumulation of misfolded/unfolded proteins in the ER is accompanied by alterations in ER Ca²⁺ homeostasis. Furthermore, familial AD mutations in PSs, components of the γ -secretase complex involved in A β production [54], have been linked to the perturbation of Ca²⁺ homeostasis [55-57]. For instance, PS1 holoprotein seems to form a complex with the SERCA channel and contribute to the regulation of ER Ca²⁺ levels [58]. Consequently, alterations in PSs that impair the formation of ER Ca²⁺ leak channels causes neurodegeneration independent of γ -secretase activity [56]. It was also found that some sporadic AD brains preferentially express an alternative splicing form of PS2 (lacking exon 5) compared with those of age-matched controls [59]. When ER Ca²⁺ levels decrease, the Ca²⁺-dependent chaperones cannot function properly and misfolded/unfolded proteins accumulate within the ER activating the UPR [60]. Alteration of intracellular Ca²⁺ concentration, reactive oxygen species, blocked ER-to-Golgi transport, inhibition of protein degradation, decrease in ATP levels and other insults may also cause ER stress and release of Ca²⁺ from the ER lumen into the cytoplasm [61]. Previously, we demonstrated in primary cultured neurons that A β induces the release of Ca²⁺ from the ER leading to cytosolic Ca²⁺ rise and activation of apoptotic cell death [38]. Here, ER Ca²⁺ content was shown to be decreased in brain ECs, and to be followed by a significant increase in cytosolic Ca²⁺ levels upon A β ₁₋₄₀ exposure. These findings are in accordance with the results obtained by Kito and co-workers who demonstrated, in another brain EC line, that ER stress increases intracellular Ca²⁺ levels [47].

The release of Ca²⁺ from ER and consequent increase in cytosolic Ca²⁺ levels can activate pathways that culminate in apoptosis [62-64]. Deregulation of the BBB is a primary event in AD, which occurs before neuronal loss that underlies the prominent brain atrophy found in the brain of patients [5, 65]. The activation of apoptosis in the brain of AD patients is a controversial issue, but several studies found activation of caspase-3 in AD patients [66]. Additionally, recent studies also show apoptosis in vascular cells in AD patients [67]. Furthermore, several in vitro studies found that A β induces apoptosis in neurons, ECs, pericytes, and other brain cells [38, 68, 69]. Moreover, cerebrovascular accumulation of A β in mice was shown to induce apoptotic cell death in ECs [8]. In our previous studies, we demonstrated the involvement of

ER Ca^{2+} release induced by different $\text{A}\beta$ peptides in mitochondria-mediated apoptosis in cortical neurons and AD cybrids [28, 38, 70]. Thapsigargin-mediated perturbation in Ca^{2+} homeostasis was shown to lead to apoptosis in a cross-talk between the death receptor and mitochondrial pathways [71]. Ca^{2+} channels associated with the ER ryanodine receptor (RyR) are involved in Ca^{2+} homeostasis and control ER-to-mitochondria Ca^{2+} transfer [72]. The prevention of $\text{A}\beta_{1-40}$ -induced decrease in $\Delta\psi_{\text{mit}}$ promoted by dantrolene, an RyR inhibitor, demonstrates the involvement of Ca^{2+} released from the ER in mitochondrial membrane depolarization and consequent induction of mitochondria-dependent apoptosis in ECs. After prolonged or intense activation of UPR and perturbation of ER Ca^{2+} homeostasis, the pro-apoptotic transcription factor CHOP/GADD153 can be upregulated [24, 73]. In turn, CHOP/GADD153 upregulates the pro-apoptotic BH3-only protein Bim [74], inhibits the transcription of the anti-apoptotic Bcl-2 protein and induces the translocation of Bax to mitochondria and the subsequent cytochrome c release and activation of caspase-9 and -3, finally leading to apoptosis [26, 75]. Therefore, the reduction in ER Ca^{2+} content, as well as the activation of ER stress and the consequent augment of CHOP/GADD153 protein levels can induce mitochondria-mediated apoptosis thus explaining the decrease in cells viability and the increase in the number of apoptotic cells observed after $\text{A}\beta_{1-40}$ treatment. To confirm this hypothesis, Bcl-2, Bax, and cytochrome c protein levels were analyzed in mitochondrial and cytosolic fractions of RBE4 cells and $\Delta\psi_{\text{mit}}$ was measured. The Bax/Bcl-2 ratio, which could be used to predict mitochondria-mediated apoptosis, increased in mitochondria, especially due to an increase of Bax levels, and decreased in cytosol in $\text{A}\beta_{1-40}$ -treated cells, suggesting that $\text{A}\beta_{1-40}$ induces the translocation of Bax to mitochondria. Bax can form pores in the mitochondrial membrane permitting the release of ions and consequently decrease in $\Delta\psi_{\text{mit}}$. Moreover, cytochrome c can be released from mitochondria and induce apoptosis. Accordingly, cytochrome c levels were significantly decreased in mitochondria and increased in cytosol after incubation with $\text{A}\beta_{1-40}$ and the downstream caspase-9 was shown to be activated under these conditions. Furthermore, the activity of caspase-3 increased upon $\text{A}\beta_{1-40}$ treatment leading to the cleavage of PARP1, a DNA repair enzyme [76]. These alterations in pro-apoptotic mediators follow changes in ER and cytosolic Ca^{2+} homeostasis, ER stress markers and precede the decrease in cell viability and the increase in the number of apoptotic cells suggesting that $\text{A}\beta_{1-40}$ activates a

mitochondrial-mediated apoptotic cell death pathway triggered by ER stress in brain ECs. During prolonged ER stress, the ER membrane resident caspase-12 can be activated subsequently initiating a mitochondria-independent caspase cascade that finally leads to apoptosis [17]. Caspase-12 is activated under ER stress conditions, including disruption of ER Ca^{2+} homeostasis and excessive accumulation of proteins in ER lumen, but not by membrane- or mitochondrial-targeted apoptotic signals [77]. Additionally, the increase in cytosolic Ca^{2+} levels resulting from ER stress activates calpains that in turn activate the murine caspase-12 [78, 79]. However, UPR induction in the absence of caspase-12 activation has also been previously found in ECs [80]. In this work, the protein levels of caspase-12 were significantly increased in $\text{A}\beta_{1-40}$ -treated ECs together with an increase in caspase-12-like activity, which reached maximal activation at 12 hr of incubation. Caspase-12 can activate caspase-9 (in an Apaf-1 and cytochrome c independent manner) that in turn activates the apoptosis effector caspase-3 [78]. $\text{A}\beta_{1-40}$ activated both caspase-3 and -9 after 6 and 12hr incubation. These results support that $\text{A}\beta$ -induced ER stress triggers apoptotic cell death in brain ECs also by mitochondria-independent cell death pathways.

In this study, caspase-12 activation and Bax translocation into mitochondria and subsequent cytochrome c release and caspases-9 and -3 activation have a maximum increase 12 hr after $\text{A}\beta_{1-40}$ treatment but decreased at 24 hr. However, cell viability continues to decrease and the number of apoptotic cells continues to increase at 24 hr of incubation. These findings suggest that alternative mechanisms must be implicated in the compromise in cell survival and significant apoptotic cell death at later stages (24 hr). It is known that $\text{A}\beta$ in brain patients with AD excessively increase PARP1 activity, also present in mitochondria, leading to the accumulation of poly(ADP-ribose) that in turn induces the release of AIF from mitochondria and consequent translocation to the nucleus [81]. Furthermore, activation of calpains after increase in cytosolic Ca^{2+} , alterations in $\Delta\psi_{\text{mit}}$ and the formation of pores in mitochondrial membrane by Bax or other pro-apoptotic Bcl-2 family member could also promote AIF release from mitochondria and its nuclear translocation [82, 83]. In the nucleus, AIF leads to chromatin condensation and DNA fragmentation and triggers caspases-independent apoptosis [84]. Accordingly, treatment of RBE4 cells with $\text{A}\beta_{1-40}$ for 24 hr increased the levels of AIF in the nucleus. The AIF-mediated apoptosis can partially explain the differences in the percentage of cell

death measured by the TUNEL assay versus Hoechst 33342/PI since the morphology of the nucleus during apoptosis induced by AIF is not easily discriminated from that of controls [84].

The ER is a key regulator of several cellular processes and therefore its dysfunction might compromise seriously cell survival [85]. The activation of the UPR is a protective mechanism to counteract ER stress and re-establish homeostasis. However, when ER stress is prolonged or too severe, apoptotic cell death is induced, which can occur through different mechanisms (CHOP upregulation, caspase-12 activation, JNK activation,...)[86]. Since the ER sensors IRE1, ATF6 and PERK and downstream UPR signalling pathways are implicated in both cell survival and death, ER stress inhibitors can prevent ER stress-induced cell death but can also interfere with cell survival pathways and impair the numerous ER-dependent cellular functions. For that reason, we do not expect that strategies to prevent UPR activation can revert the toxic A β effects, since loss of protective pathways will turn cells more sensitive to stress. Accordingly, we tested several ER stress inhibitors such as TUDCA (tauroursodeoxycholic acid), PBA (4-phenylbutyric acid), VPA (valproic acid sodium), alone or in combination, in ECs treated with two well known ER stress inducers, thapsigargin and brefeldin A, or with A β and we were not succeeded in protecting cells from ER stress-induced apoptosis (data not shown). In addition, we can not exclude the activation of ER-independent cell death pathways by A β , which are not rescued by ER stress inhibitors. Finally, the increases in the levels of CHOP and caspase-12, as well as in caspase-12 activity in A β -treated ECs, support that this peptide induces an ER stress-mediated apoptotic cell death pathway.

5. Conclusion

In conclusion, our findings support that vascular alterations in AD arise from the deleterious effects of A β ₁₋₄₀ on brain ECs that activate cell death pathways through the perturbation of ER Ca²⁺ homeostasis and induction of ER stress (Fig. 8). These evidences could contribute to the development of novel therapeutic strategies targeting the ER to prevent or delay the progression of AD.

6. Acknowledgements

The authors are grateful to Dr. Jon Holy (University of Minnesota, Duluth, USA) for the generous gift of RBE4 cells and to Luísa Cortes for microscopy assistance. This work was supported by 'Fundação para a Ciência e a Tecnologia' (FCT), Portugal (the project PEst-C/SAU/LA0001/2011, PhD fellowship attributed to AC Fonseca: SFRH/BD/47573/2008 and post-doc fellowship attributed to E Ferreira: SFRH / BPD/43536/2008) and 'Instituto de Investigação Interdisciplinar', University of Coimbra, Portugal (project nº III/40/2008).

7. Disclosure statement

The authors declare that this work was conducted without financial or commercial relationships that could be considering as a potential conflict of interest.

8. References

- [1] E. Karran, M. Mercken, B. De Strooper, The amyloid cascade hypothesis for Alzheimer's disease: an appraisal for the development of therapeutics, *Nat Rev Drug Discov*, 10 (2011) 698-712.
- [2] B.V. Zlokovic, Neurovascular pathways to neurodegeneration in Alzheimer's disease and other disorders, *Nature reviews*, 12 (2011) 723-738.
- [3] D. Knopman, R. Roberts, Vascular risk factors: imaging and neuropathologic correlates, *J Alzheimers Dis*, 20 (2010) 699-709.
- [4] D. Dickstein, J. Walsh, H. Brautigam, S.J. Stockton, S. Gandy, P. Hof, Role of vascular risk factors and vascular dysfunction in Alzheimer's disease, *Mt Sinai J Med*, 77 (2010) 82-102.
- [5] C. Iadecola, Neurovascular regulation in the normal brain and in Alzheimer's disease, *Nature reviews*, 5 (2004) 347-360.
- [6] G.W. Small, L.M. Ercoli, D.H. Silverman, S.C. Huang, S. Komo, S.Y. Bookheimer, H. Lavretsky, K. Miller, P. Siddarth, N.L. Rasgon, J.C. Mazziotta, S. Saxena, H.M. Wu, M.S. Mega, J.L. Cummings, A.M. Saunders, M.A. Pericak-Vance, A.D. Roses, J.R. Barrio, M.E. Phelps, Cerebral metabolic and cognitive decline in persons at genetic risk for Alzheimer's disease, *Proceedings of the National Academy of Sciences of the United States of America*, 97 (2000) 6037-6042.
- [7] J. Attems, H. Yamaguchi, T.C. Saido, D.R. Thal, Capillary CAA and perivascular Abeta-deposition: two distinct features of Alzheimer's disease pathology, *Journal of the neurological sciences*, 299 (2010) 155-162.
- [8] J. Miao, F. Xu, J. Davis, I. Otte-Holler, M.M. Verbeek, W.E. Van Nostrand, Cerebral microvascular amyloid beta protein deposition induces vascular degeneration and neuroinflammation in transgenic mice expressing human vasculotropic mutant amyloid beta precursor protein, *Am J Pathol*, 167 (2005) 505-515.
- [9] M.J. Hsu, J.R. Sheu, C.H. Lin, M.Y. Shen, C.Y. Hsu, Mitochondrial mechanisms in amyloid beta peptide-induced cerebrovascular degeneration, *Biochimica et biophysica acta*, 1800 (2010) 290-296.
- [10] M. Gentile, C. Vecchione, A. Maffei, A. Aretini, G. Marino, R. Poulet, L. Capobianco, G. Selvetella, G. Lembo, Mechanisms of soluble beta-amyloid impairment of endothelial function, *J Biol Chem*, 279 (2004) 48135-48142.
- [11] E. Kouznetsova, M. Klingner, D. Sorger, O. Sabri, U. Grossmann, J. Steinbach, M. Scheunemann, R. Schliebs, Developmental and amyloid plaque-related changes in cerebral cortical capillaries in transgenic Tg2576 Alzheimer mice, *Int J Dev Neurosci*, 24 (2006) 187-193.
- [12] M. Chisari, S. Merlo, M. Sortino, S. Salomone, Long-term incubation with beta-amyloid peptides impairs endothelium-dependent vasodilatation in isolated rat basilar artery, *Pharmacol Res*, 61 (2010) 157-161.

- [13] S. Yang, D. Bae, H. Kang, B. Gwag, Y. Gho, C. Chae, Co-accumulation of vascular endothelial growth factor with beta-amyloid in the brain of patients with Alzheimer's disease, *Neurobiol Aging*, 25 (2004) 283-290.
- [14] S. Hayashi, N. Sato, A. Yamamoto, Y. Ikegame, S. Nakashima, T. Ogihara, R. Morishita, Alzheimer disease-associated peptide, amyloid beta40, inhibits vascular regeneration with induction of endothelial autophagy, *Arterioscler Thromb Vasc Biol*, 29 (2009) 1909-1915.
- [15] D. Luo, Y. He, H. Zhang, L. Yu, H. Chen, Z. Xu, S. Tang, F. Urano, W. Min, AIP1 is critical in transducing IRE1-mediated endoplasmic reticulum stress response, *J Biol Chem*, 283 (2008) 11905-11912.
- [16] N. Bouvier, J.P. Flinois, J. Gilleron, F.L. Sauvage, C. Legendre, P. Beaune, E. Thervet, D. Anglicheau, N. Pallet, Cyclosporine triggers endoplasmic reticulum stress in endothelial cells: a role for endothelial phenotypic changes and death, *Am J Physiol Renal Physiol*, 296 (2009) F160-169.
- [17] J.H. Lin, P. Walter, T.S. Yen, Endoplasmic reticulum stress in disease pathogenesis, *Annual review of pathology*, 3 (2008) 399-425.
- [18] Y. Kimata, K. Kohno, Endoplasmic reticulum stress-sensing mechanisms in yeast and mammalian cells, *Current opinion in cell biology*, 23 (2011) 135-142.
- [19] T. Katayama, K. Imaizumi, T. Manabe, J. Hitomi, T. Kudo, M. Tohyama, Induction of neuronal death by ER stress in Alzheimer's disease, *J Chem Neuroanat*, 28 (2004) 67-78.
- [20] K. Ameri, A.L. Harris, Activating transcription factor 4, *The international journal of biochemistry & cell biology*, 40 (2008) 14-21.
- [21] R.P. Boot-Handford, M.D. Briggs, The unfolded protein response and its relevance to connective tissue diseases, *Cell and tissue research*, 339 (2010) 197-211.
- [22] M. Calfon, H. Zeng, F. Urano, J.H. Till, S.R. Hubbard, H.P. Harding, S.G. Clark, D. Ron, IRE1 couples endoplasmic reticulum load to secretory capacity by processing the XBP-1 mRNA, *Nature*, 415 (2002) 92-96.
- [23] T. Okada, H. Yoshida, R. Akazawa, M. Negishi, K. Mori, Distinct roles of activating transcription factor 6 (ATF6) and double-stranded RNA-activated protein kinase-like endoplasmic reticulum kinase (PERK) in transcription during the mammalian unfolded protein response, *The Biochemical journal*, 366 (2002) 585-594.
- [24] S. Oyadomari, M. Mori, Roles of CHOP/GADD153 in endoplasmic reticulum stress, *Cell Death Differ*, 11 (2004) 381-389.
- [25] S.J. Marciniak, C.Y. Yun, S. Oyadomari, I. Novoa, Y. Zhang, R. Jungreis, K. Nagata, H.P. Harding, D. Ron, CHOP induces death by promoting protein synthesis and oxidation in the stressed endoplasmic reticulum, *Genes & development*, 18 (2004) 3066-3077.
- [26] R. Kim, M. Emi, K. Tanabe, S. Murakami, Role of the unfolded protein response in cell death, *Apoptosis*, 11 (2006) 5-13.
- [27] C. Giorgi, D. De Stefani, A. Bononi, R. Rizzuto, P. Pinton, Structural and functional link between the mitochondrial network and the endoplasmic reticulum, *The international journal of biochemistry & cell biology*, 41 (2009) 1817-1827.
- [28] E. Ferreira, C.R. Oliveira, C.M.F. Pereira, The release of calcium from the endoplasmic reticulum induced by amyloid-beta and prion peptides activates the mitochondrial apoptotic pathway, *Neurobiol Dis*, 30 (2008) 331-342.
- [29] J.J.M. Hoozemans, R. Veerhuis, E.S.V. Haastert, J.M. Rozemuller, F. Baas, P. Eikelenboom, W. Scheper, The unfolded protein response is activated in Alzheimer's disease, *Acta Neuropathol*, 110 (2005) 165-172.
- [30] S. Song, H. Lee, T. Kam, M. Tai, J. Lee, J. Noh, S. Shim, S. Seo, Y. Kong, T. Nakagawa, C. Chung, D. Choi, H. Oubrahim, Y. Jung, E2-25K/Hip-2 regulates caspase-12 in ER stress-mediated Abeta neurotoxicity, *J Cell Biol*, 182 (2008) 675-684.
- [31] Z. Ling, Q. Tian, L. Wang, Z. Fu, X. Wang, Q. Wang, J. Wang, Constant illumination induces Alzheimer-like damages with endoplasmic reticulum involvement and the protection of melatonin, *J Alzheimers Dis*, 16 (2009) 287-300.
- [32] F. Yukioka, S. Matsuzaki, K. Kawamoto, Y. Koyama, J. Hitomi, T. Katayama, M. Tohyama, Presenilin-1 mutation activates the signaling pathway of caspase-4 in endoplasmic reticulum stress-induced apoptosis, *Neurochemistry international*, 52 (2008) 683-687.
- [33] C. Supnet, I. Bezprozvanny, Presenilins function in ER calcium leak and Alzheimer's disease pathogenesis, *Cell Calcium*, 50 (2011) 303-309.
- [34] T. Hoshino, T. Nakaya, W. Araki, K. Suzuki, T. Suzuki, T. Mizushima, Endoplasmic reticulum chaperones inhibit the production of amyloid-beta peptides, *The Biochemical journal*, 402 (2007) 581-589.

- [35] Y. Yang, R.S. Turner, J.R. Gaut, The chaperone BiP/GRP78 binds to amyloid precursor protein and decreases Abeta40 and Abeta42 secretion, *J Biol Chem*, 273 (1998) 25552-25555.
- [36] N. Sato, K. Imaizumi, T. Manabe, M. Taniguchi, J. Hitomi, T. Katayama, T. Yoneda, T. Morihara, Y. Yasuda, T. Takagi, T. Kudo, T. Tsuda, Y. Itoyama, T. Makifuchi, P.E. Fraser, P. St George-Hyslop, M. Tohyama, Increased production of beta-amyloid and vulnerability to endoplasmic reticulum stress by an aberrant spliced form of presenilin 2, *J Biol Chem*, 276 (2001) 2108-2114.
- [37] E. Ferreira, R. Resende, R. Costa, C.R. Oliveira, C.M.F. Pereira, An endoplasmic-reticulum-specific apoptotic pathway is involved in prion and amyloid-beta peptides neurotoxicity, *Neurobiol Dis*, 23 (2006) 669-678.
- [38] R. Resende, E. Ferreira, C. Pereira, C.R. Oliveira, Neurotoxic effect of oligomeric and fibrillar species of A β 1-42 peptide: involvement of endoplasmic reticulum calcium release in oligomers-induced cell death, *Neuroscience*, 155 (2008) 725-737.
- [39] P.A. Adlard, B.J. Cummings, Alzheimer's disease--a sum greater than its parts?, *Neurobiol Aging*, 25 (2004) 725-733; discussion 743-746.
- [40] P.O. Couraud, J. Greenwood, F. Roux, P. Adamson, Development and characterization of immortalized cerebral endothelial cell lines, *Methods in molecular medicine*, 89 (2003) 349-364.
- [41] C. Pereira, M.S. Santos, C. Oliveira, Involvement of oxidative stress on the impairment of energy metabolism induced by A beta peptides on PC12 cells: protection by antioxidants, *Neurobiol Dis*, 6 (1999) 209-219.
- [42] C.M. Pereira, C.R. Oliveira, Glutamate toxicity on a PC12 cell line involves glutathione (GSH) depletion and oxidative stress, *Free Radic Biol Med*, 23 (1997) 637-647.
- [43] C. Bandeira-Duarte, C. Carvalho, J.E. Cragoe, A. Carvalho, Influence of isolation media on synaptosomal properties: intracellular pH, pCa, and Ca²⁺ uptake, *Neurochem Res*, 15 (1990) 313-320.
- [44] P. Garção, C.R. Oliveira, P. Agostinho, Comparative study of microglia activation induced by amyloid-beta and prion peptides: role in neurodegeneration, *J Neurosci Res*, 84 (2006) 182-193.
- [45] M. Sheikh-Ali, S. Sultan, A.R. Alamir, M.J. Haas, A.D. Mooradian, Effects of antioxidants on glucose-induced oxidative stress and endoplasmic reticulum stress in endothelial cells, *Diabetes research and clinical practice*, 87 (2010) 161-166.
- [46] T. Adachi, H. Yasuda, S. Nakamura, T. Kamiya, H. Hara, H. Hara, T. Ikeda, Endoplasmic reticulum stress induces retinal endothelial permeability of extracellular-superoxide dismutase, *Free Radic Res*, 45 (2011) 1083-1092.
- [47] H. Kito, D. Yamazaki, S. Ohya, H. Yamamura, K. Asai, Y. Imaizumi, Up-regulation of K(ir)2.1 by ER stress facilitates cell death of brain capillary endothelial cells, *Biochem Biophys Res Commun*, 411 (2011) 293-298.
- [48] C. Reitz, C. Brayne, R. Mayeux, Epidemiology of Alzheimer disease, *Nat Rev Neurol*, 7 (2011) 137-152.
- [49] S. Takeda, N. Sato, K. Uchio-Yamada, K. Sawada, T. Kunieda, D. Takeuchi, H. Kurinami, M. Shinohara, H. Rakugi, R. Morishita, Diabetes-accelerated memory dysfunction via cerebrovascular inflammation and Abeta deposition in an Alzheimer mouse model with diabetes, *Proceedings of the National Academy of Sciences of the United States of America*, 107 (2010) 7036-7041.
- [50] G.S. Hotamisligil, Endoplasmic reticulum stress and the inflammatory basis of metabolic disease, *Cell*, 140 (2010) 900-917.
- [51] S. Fossati, J. Ghiso, A. Rostagno, TRAIL death receptors DR4 and DR5 mediate cerebral microvascular endothelial cell apoptosis induced by oligomeric Alzheimer's Abeta, *Cell death & disease*, 3 (2012) e321.
- [52] R. Deane, Z. Wu, B.V. Zlokovic, RAGE (yin) versus LRP (yang) balance regulates alzheimer amyloid beta-peptide clearance through transport across the blood-brain barrier, *Stroke; a journal of cerebral circulation*, 35 (2004) 2628-2631.
- [53] O. Ghribi, The role of the endoplasmic reticulum in the accumulation of beta-amyloid peptide in Alzheimer's disease, *Current molecular medicine*, 6 (2006) 119-133.
- [54] C. Żekanowski, D. Religa, C. Graff, S. Filipek, J. Kuźnicki, Genetic aspects of Alzheimer's disease, *Acta Neurobiol Exp*, 64 (2004) 19-31.
- [55] F.M. LaFerla, Calcium dyshomeostasis and intracellular signalling in Alzheimer's disease, *Nature reviews*, 3 (2002) 862-872.
- [56] H. Tu, O. Nelson, A. Bezprozvanny, Z. Wang, S.F. Lee, Y.H. Hao, L. Serneels, B. De Strooper, G. Yu, I. Bezprozvanny, Presenilins form ER Ca²⁺ leak channels, a function disrupted by familial Alzheimer's disease-linked mutations, *Cell*, 126 (2006) 981-993.

- [57] M.A. Leissring, Y. Akbari, C.M. Fanger, M.D. Cahalan, M.P. Mattson, F.M. LaFerla, Capacitative calcium entry deficits and elevated luminal calcium content in mutant presenilin-1 knockin mice, *J Cell Biol*, 149 (2000) 793-798.
- [58] H. Jin, N. Sanjo, T. Uchihara, K. Watabe, P. St George-Hyslop, P.E. Fraser, H. Mizusawa, Presenilin-1 holoprotein is an interacting partner of sarco endoplasmic reticulum calcium-ATPase and confers resistance to endoplasmic reticulum stress, *J Alzheimers Dis*, 20 (2010) 261-273.
- [59] N. Sato, O. Hori, A. Yamaguchi, J.C. Lambert, M.C. Chartier-Harlin, P.A. Robinson, A. Delacourte, A.M. Schmidt, T. Furuyama, K. Imaizumi, M. Tohyama, T. Takagi, A novel presenilin-2 splice variant in human Alzheimer's disease brain tissue, *Journal of neurochemistry*, 72 (1999) 2498-2505.
- [60] M. Michalak, J.M. Robert Parker, M. Opas, Ca²⁺ signaling and calcium binding chaperones of the endoplasmic reticulum, *Cell Calcium*, 32 (2002) 269-278.
- [61] M. Schröder, Endoplasmic reticulum stress responses, *Cell Mol Life Sci*, 65 (2008) 862-694.
- [62] C. Supnet, I. Bezprozvanny, The dysregulation of intracellular calcium in Alzheimer disease, *Cell Calcium*, 47 (2010) 183-189.
- [63] J.T. Yu, R.C. Chang, L. Tan, Calcium dysregulation in Alzheimer's disease: from mechanisms to therapeutic opportunities, *Progress in neurobiology*, 89 (2009) 240-255.
- [64] J.M. Timmins, L. Ozcan, T.A. Seimon, G. Li, C. Malagelada, J. Backs, T. Backs, R. Bassel-Duby, E.N. Olson, M.E. Anderson, I. Tabas, Calcium/calmodulin-dependent protein kinase II links ER stress with Fas and mitochondrial apoptosis pathways, *The Journal of clinical investigation*, 119 (2009) 2925-2941.
- [65] K.K. Leung, J.W. Bartlett, J. Barnes, E.N. Manning, S. Ourselin, N.C. Fox, Cerebral atrophy in mild cognitive impairment and Alzheimer disease: rates and acceleration, *Neurology*, 80 (2013) 648-654.
- [66] S. Snigdha, E.D. Smith, G.A. Prieto, C.W. Cotman, Caspase-3 activation as a bifurcation point between plasticity and cell death, *Neuroscience bulletin*, 28 (2012) 14-24.
- [67] S. Xue, X. Cai, W. Li, Z. Zhang, W. Dong, G. Hui, Elevated plasma endothelial microparticles in Alzheimer's disease, *Dementia and geriatric cognitive disorders*, 34 (2012) 174-180.
- [68] M.M. Verbeek, R.M. de Waal, J.J. Schipper, W.E. Van Nostrand, Rapid degeneration of cultured human brain pericytes by amyloid beta protein, *Journal of neurochemistry*, 68 (1997) 1135-1141.
- [69] J. Davis, D.H. Cribbs, C.W. Cotman, W.E. Van Nostrand, Pathogenic amyloid beta-protein induces apoptosis in cultured human cerebrovascular smooth muscle cells, *Amyloid*, 6 (1999) 157-164.
- [70] R.O. Costa, E. Ferreira, I. Martins, I. Santana, S.M. Cardoso, C.R. Oliveira, C.M. Pereira, Amyloid beta-induced ER stress is enhanced under mitochondrial dysfunction conditions, *Neurobiol Aging*, 33 (2012) 824 e825-816.
- [71] Q. He, D.I. Lee, R. Rong, M. Yu, X. Luo, M. Klein, W.S. El-Deiry, Y. Huang, A. Hussain, M.S. Sheikh, Endoplasmic reticulum calcium pool depletion-induced apoptosis is coupled with activation of the death receptor 5 pathway, *Oncogene*, 21 (2002) 2623-2633.
- [72] N.K. Woods, J. Padmanabhan, Neuronal calcium signaling and Alzheimer's disease, *Advances in experimental medicine and biology*, 740 (2012) 1193-1217.
- [73] J.D. Malhotra, R.J. Kaufman, The endoplasmic reticulum and the unfolded protein response, *Seminars in cell & developmental biology*, 18 (2007) 716-731.
- [74] H. Puthalakath, L.A. O'Reilly, P. Gunn, L. Lee, P.N. Kelly, N.D. Huntington, P.D. Hughes, E.M. Michalak, J. McKimm-Breschkin, N. Motoyama, T. Gotoh, S. Akira, P. Bouillet, A. Strasser, ER stress triggers apoptosis by activating BH3-only protein Bim, *Cell*, 129 (2007) 1337-1349.
- [75] J.S. Pober, W. Min, J.R. Bradley, Mechanisms of endothelial dysfunction, injury, and death, *Annual review of pathology*, 4 (2009) 71-95.
- [76] G.V. Chaitanya, A.J. Steven, P.P. Babu, PARP-1 cleavage fragments: signatures of cell-death proteases in neurodegeneration, *Cell Commun Signal*, 8 (2010) 31.
- [77] T. Nakagawa, H. Zhu, N. Morishima, E. Li, J. Xu, B.A. Yankner, J. Yuan, Caspase-12 mediates endoplasmic-reticulum-specific apoptosis and cytotoxicity by amyloid-beta, *Nature*, 403 (2000) 98-103.
- [78] L. Moretti, Y.I. Cha, K.J. Niermann, B. Lu, Switch between apoptosis and autophagy: radiation-induced endoplasmic reticulum stress?, *Cell cycle (Georgetown, Tex)*, 6 (2007) 793-798.
- [79] S. Matsuzaki, T. Hiratsuka, R. Kuwahara, T. Katayama, M. Tohyama, Caspase-4 is partially cleaved by calpain via the impairment of Ca²⁺ homeostasis under the ER stress, *Neurochemistry international*, 56 (2010) 352-256.

- [80] Y.Y. Chen, M.Z. Zheng, P.P. Lv, L. Hu, L.L. Wang, Y.L. Shen, Hydrogen peroxide regulates glucose-regulated protein 78 expression via a cyclooxygenase-2 dependent mechanism, *Journal of biochemical and molecular toxicology*, 24 (2010) 279-285.
- [81] J.B. Strosznajder, G.A. Czapski, A. Adamczyk, R.P. Strosznajder, Poly(ADP-ribose) Polymerase-1 in Amyloid Beta Toxicity and Alzheimer's Disease, *Molecular neurobiology*, 46 (2012) 78-84.
- [82] B.M. Polster, G. Basanez, A. Etxebarria, J.M. Hardwick, D.G. Nicholls, Calpain I induces cleavage and release of apoptosis-inducing factor from isolated mitochondria, *J Biol Chem*, 280 (2005) 6447-6454.
- [83] E. Er, L. Oliver, P.F. Cartron, P. Juin, S. Manon, F.M. Vallette, Mitochondria as the target of the pro-apoptotic protein Bax, *Biochimica et biophysica acta*, 1757 (2006) 1301-1311.
- [84] E. Ulukaya, C. Acilan, Y. Yilmaz, Apoptosis: why and how does it occur in biology?, *Cell biochemistry and function*, 29 (2011) 468-480.
- [85] F. Engin, G.S. Hotamisligil, Restoring endoplasmic reticulum function by chemical chaperones: an emerging therapeutic approach for metabolic diseases, *Diabetes, obesity & metabolism*, 12 Suppl 2 (2010) 108-115.
- [86] A.M. Gorman, S.J. Healy, R. Jager, A. Samali, Stress management at the ER: regulators of ER stress-induced apoptosis, *Pharmacology & therapeutics*, 134 (2012) 306-316.

ACCEPTED MANUSCRIPT

Titles and legends to figures

Figure 1. $A\beta_{1-40}$ decreases brain endothelial cell survival activating apoptotic cell death. (A) RBE4 cells treated with $2.5 \mu\text{M}$ $A\beta_{1-40}$ for 3 hr were stained with ThS to detect β -sheet $A\beta$ species and observed with 400x amplification in a confocal microscope. (B) Additionally, cells were treated with 0.1 or $2.5 \mu\text{M}$ $A\beta_{1-40}$ for 3, 6, 12, or 24 hr and cell viability was evaluated by the MTT assay. Data correspond to the percentage of the absorbance determined under control conditions (untreated cells). (C) Moreover, RBE4 cells were incubated for 6 or 24 hr with $2.5 \mu\text{M}$ $A\beta_{1-40}$ and the release of LDH was measured to monitor necrosis-associated loss of plasma membrane integrity. The results correspond to the percentage of LDH released to the extracellular medium and are presented relative to control. (D-G) Furthermore, cells were incubated with $2.5 \mu\text{M}$ $A\beta_{1-40}$ for 24 hr and the number of apoptotic and necrotic cells was measured with Hoechst 33342/PI staining (D and E) or by the TUNEL assay (F and G). In (D) are represented the Hoechst 33342, PI and merged images and in (F) are represented the phase contrast, the fluorescence (green) and the merged images of TUNEL-stained cells visualized with 400x amplification. A minimum of 150 cells were scored for each coverslip and the number of dead cells, presented as the percentage of total number of cells (E and G), was quantified. Data represent the means \pm SEM of at least three independent experiments performed in duplicate. *** $p < 0.001$ significantly different from control.

Figure 2. $A\beta_{1-40}$ induces ER stress in brain endothelial cells. RBE4 cells were treated with $2.5 \mu\text{M}$ $A\beta_{1-40}$ peptide for 3, 6, 12, or 24 hr and then ATF4 (A and B), unspliced XBP-1 (A and C), spliced XBP1 (A and D), cleaved ATF6 α (A and E), and GRP78 (A and F) protein levels were quantified by WB. Proteins (15 μg) from cell lysates were separated by SDS-PAGE and immunoblotted with specific antibodies. An anti- α -tubulin antibody was applied as a protein loading control and used to normalize ER stress protein levels. The results were calculated relatively to control values and represent the means \pm SEM of at least eight independent experiments. (G and H) Additionally, cells cultured in glass coverslips were incubated with $2.5 \mu\text{M}$ $A\beta_{1-40}$ for 6hr and the nuclear localization of ATF6 α was analyzed by immunocytochemistry using an antibody against ATF6 α and Hoechst 33342 to label nuclei. (G) Fluorescence images of control and treated cells were

visualized with 630x amplification in a confocal microscope. (H) The ATF6 α staining in the nucleus of a minimum of 100 cells for each coverslip was measured using the WCIF ImageJ program. Results were calculated as the means \pm SEM of at least three independent experiments performed in duplicate and were normalized to control values. * $p < 0.05$, ** $p < 0.01$, and *** $p < 0.001$ significantly different from control.

Figure 3. ER and cytosolic Ca²⁺ content is affected in A β ₁₋₄₀-treated brain endothelial cells. (A) The fluorescence ratio at 340/380 nm of the Ca²⁺-sensitive probe Fura-2/AM was monitored in the absence of external Ca²⁺ in controls and in cells treated with A β ₁₋₄₀ for 3 or 24 hr. After establishment of a basal fluorescence signal, 2.5 μ M thapsigargin was added to deplete ER Ca²⁺ content. A representative experiment is presented in. (B) The peak amplitude of Fura-2 fluorescence was used to evaluate ER Ca²⁺ content. (C) Additionally, cytosolic Ca²⁺ levels were analyzed using the Ca²⁺ dye Indo-1/AM after treatment of RBE4 cells with 2.5 μ M A β ₁₋₄₀ for 3, 6, 12, or 24 hr. Data were normalized to control and represent the means \pm SEM of at least three independent experiments performed in duplicate. ** $p < 0.01$ and *** $p < 0.001$ significantly different from untreated cells.

Figure 4. CHOP protein levels are increased by A β ₁₋₄₀ treatment in brain endothelial cells. RBE4 cells were treated with 2.5 μ M A β ₁₋₄₀ for 3, 6, 12, or 24 hr and then CHOP protein levels were quantified by WB. Protein (15 μ g) obtained from cell lysates was separated by SDS-PAGE and immunoblotted with the respective antibody. An anti- α -tubulin antibody was used as a protein loading control and used to normalize CHOP protein levels (A and B). The results were normalized to control and represent the means \pm SEM of at least eight independent experiments. ** $p < 0.01$ significantly different from control.

Figure 5. The mitochondria-mediated apoptotic cell death pathway is activated by A β ₁₋₄₀ in brain endothelial cells. After treatment of RBE4 cells with 2.5 μ M A β ₁₋₄₀ for 3, 6, 12, or 24 hr, mitochondrial and cytosolic extracts were prepared and proteins (30 μ g) were separated by SDS-PAGE and immunoblotted with anti-Bcl-2, anti-Bax (A, B and C), and anti-cytochrome c (A, D and E) antibodies. Anti-TBP and anti-GAPDH

antibodies were applied as protein loading control for nuclear and cytosolic fractions respectively. Bax/Bcl-2 ratio in the mitochondria (B) and in the cytosol (C) was calculated. The ratio between mitochondrial and total (cytosolic plus mitochondrial) cytochrome c levels (D) and the ratio between cytosolic and total cytochrome c levels (E) were also calculated. Additionally, the $\Delta\psi_{mit}$ was measured upon $A\beta_{1-40}$ (F) and dantolene (G) treatment of RBE4 cells using the fluorescent probe TMRM. The results were normalized to control and represent the means \pm SEM of at least five independent experiments. * $p < 0.05$, ** $p < 0.01$, and *** $p < 0.001$ significantly different from control and ### $p < 0.001$ significantly different from $A\beta_{1-40}$ treated ECs.

Figure 6. $A\beta_{1-40}$ treatment activates caspases-3, -9, and -12 in brain endothelial cells and induces PARP1 cleavage. (A-C) RBE4 cells were treated with 2.5 μ M $A\beta_{1-40}$ for 3, 6, 12, or 24 hr and then pro-caspase-12 and caspase-12 protein levels were quantified by WB. Proteins (15 μ g) obtained from cell lysates were separated by SDS-PAGE and immunoblotted with a specific antibody and an anti-GAPDH antibody applied as a protein loading control. The ratio between pro-caspase-12 (B) or caspase-12 (C) and GAPDH was calculated. The presented results were normalized to control values and represent the means \pm SEM of at least five independent experiments performed in duplicate. In addition, caspase-12 (D), caspase-9 (E), and caspase-3 (F)-like activities were determined in cell lysates using the colorimetric substrates Ac-LEVD-pNA, Ac-LEHD-pNA, and Ac-DEVD-pNA, respectively. The presented results were normalized to control and represent the means \pm SEM of at least three independent experiments performed in duplicate. (G) Moreover, RBE4 cells cultured in glass coverslips were incubated with 2.5 μ M $A\beta_{1-40}$ for 12 or 24 hr and the cleavage of PARP1 was analyzed by immunocytochemistry using an antibody against the large fragment of PARP1 resulting from caspase cleavage at Asp214 and Hoechst 33342 to label nuclei. Fluorescence images of control and treated cells were visualized with 400x amplification. * $p < 0.05$ and *** $p < 0.001$ significantly different from untreated cells.

Figure 7. $A\beta_{1-40}$ induces the translocation of AIF to the nucleus in brain endothelial cells. After treatment of RBE4 cells with 2.5 μ M $A\beta_{1-40}$ for 3, 6, 12, or 24 hr, cytosolic (A), mitochondrial (A and B) and nuclear (A and

C) extracts were prepared and proteins (30 µg) were separated by SDS-PAGE and immunoblotted with an anti-AIF antibody. Anti-GAPDH (for cytosolic fractions), anti-Tom20 (for mitochondrial fractions) and TBP (for nuclear fractions) antibodies were applied as protein loading control and used to normalize AIF protein levels. The results were normalized to control and represent the means \pm SEM of at least six independent experiments. ** $p < 0.01$ and *** $p < 0.001$ significantly different from control.

Figure 8. A β triggers apoptosis in brain endothelial cells through activation of stress responses and deregulation of Ca²⁺ homeostasis in the ER. A β induces the release of Ca²⁺ and accumulation of unfolded proteins in the endoplasmic reticulum (ER) leading to the activation of the ER stress-mediated UPR (activation of ATF6, IRE1, and PERK signalling pathways). Consequently, the transcription factors cleaved ATF6, spliced XBP-1 (sXBP-1), and ATF4 are translocated to the nucleus and induce the transcription of several genes such as the pro-apoptotic CHOP that increases the Bax/Bcl-2 ratio in mitochondria leading to the release of cytochrome c and AIF. Cytochrome c binds to Apaf-1 and activates caspase-9, which in turn activates the apoptosis effector caspase-3. On the other hand, severe ER stress is associated with massive release of Ca²⁺ from ER and activates caspase-12 that activates caspase-9 independently of Apaf-1. After translocation to the nucleus, AIF promotes chromatin condensation and DNA fragmentation resulting in apoptosis. PARP1 can repair DNA damage, however it is cleaved by caspases such as caspase-3 during apoptosis. Moreover, the Ca²⁺ released from ER is transferred to mitochondria, causing Ca²⁺ overload and decrease of mitochondrial membrane potential ($\Delta\psi_m$), leading to the release of apoptotic factors.

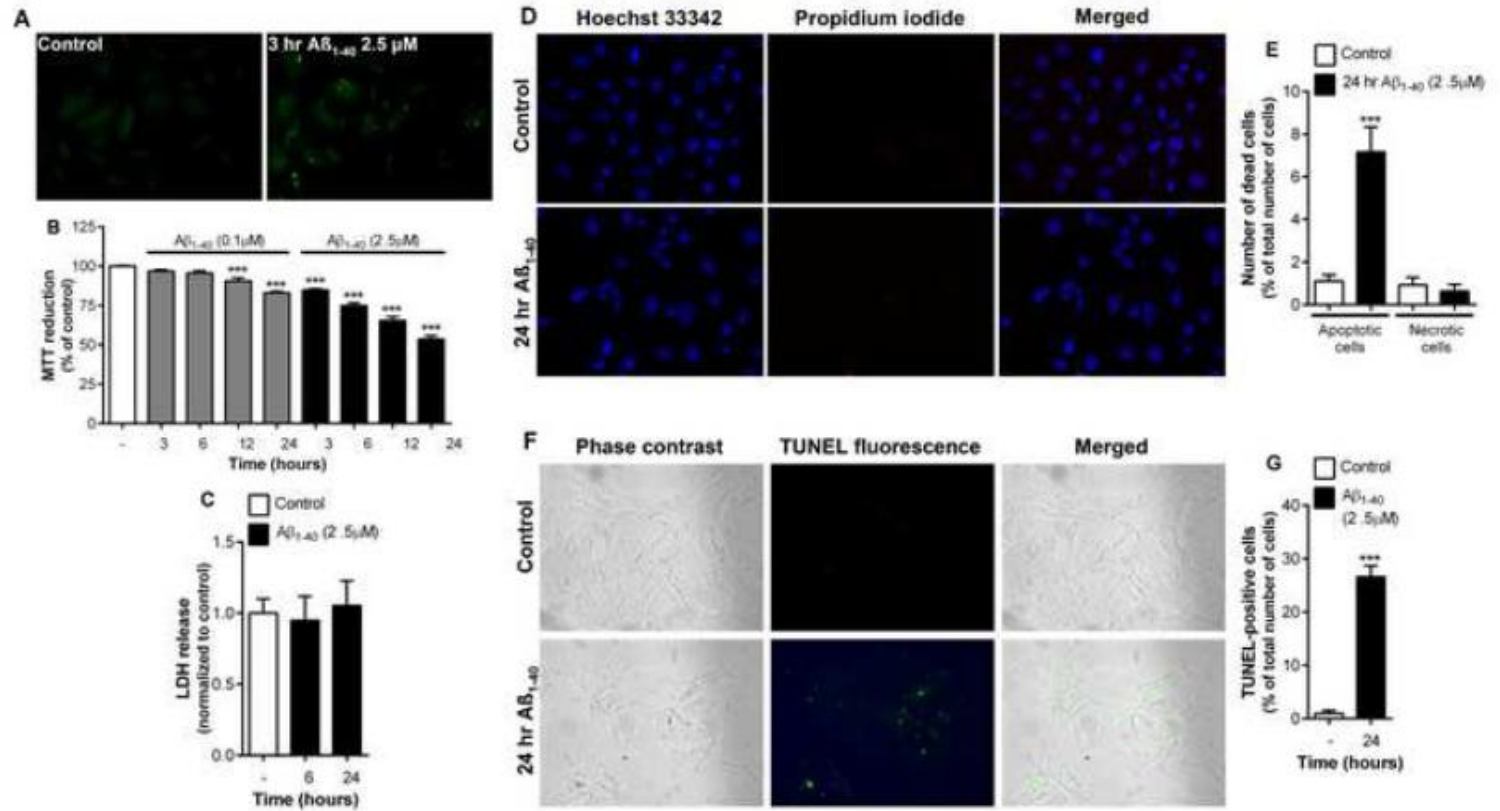


Figure 1

ACCEPTED

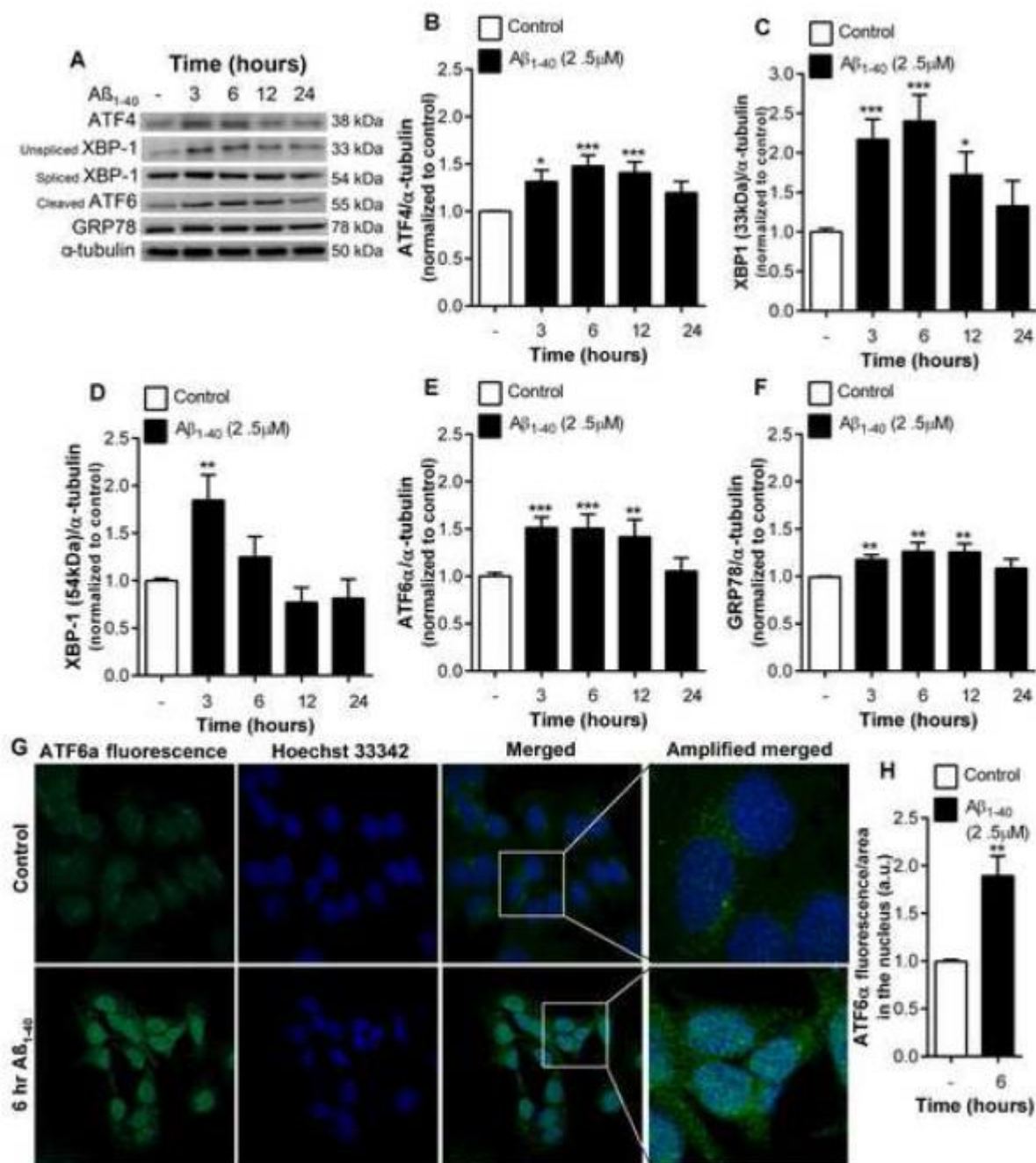


Figure 2

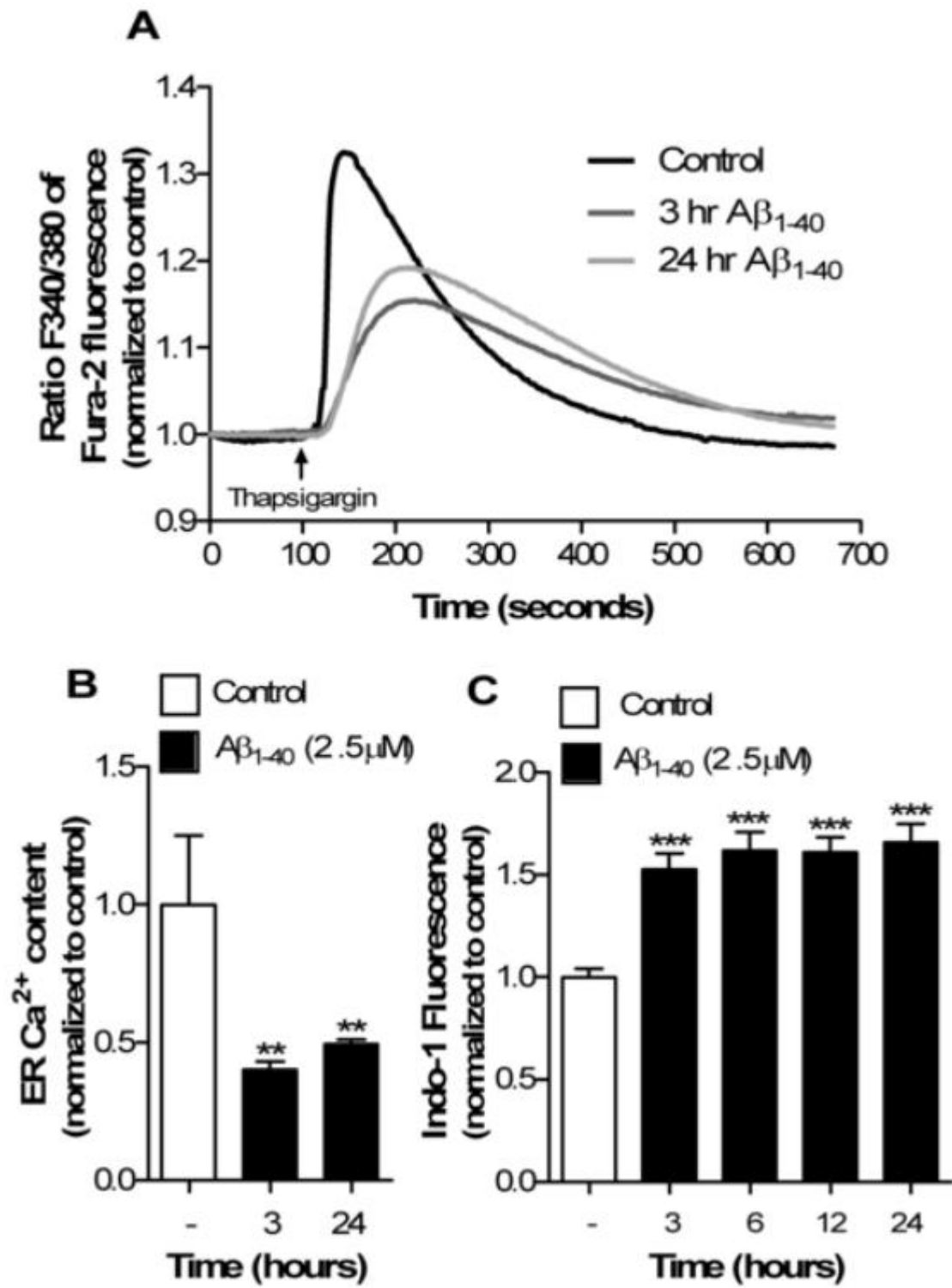


Figure 3

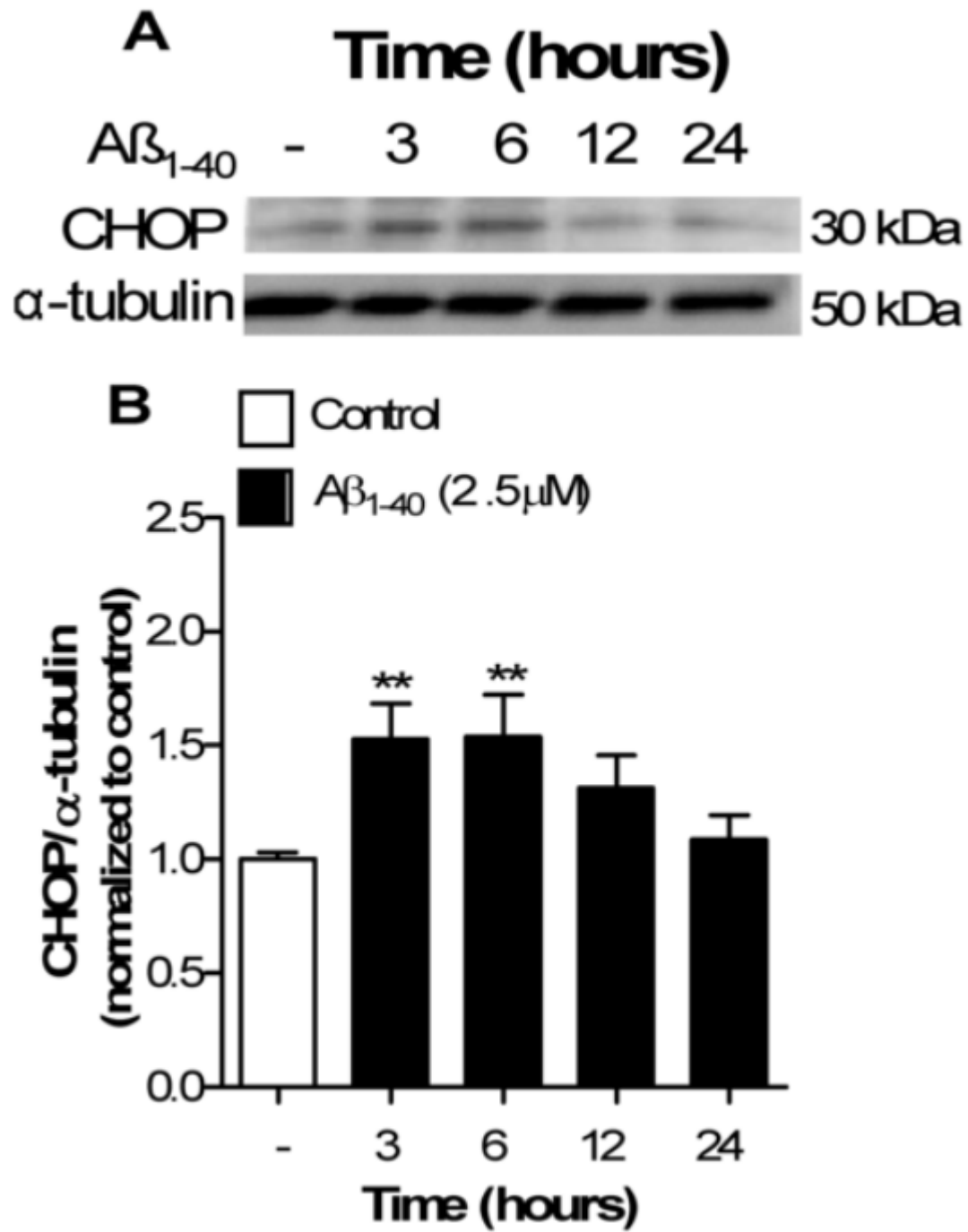


Figure 4

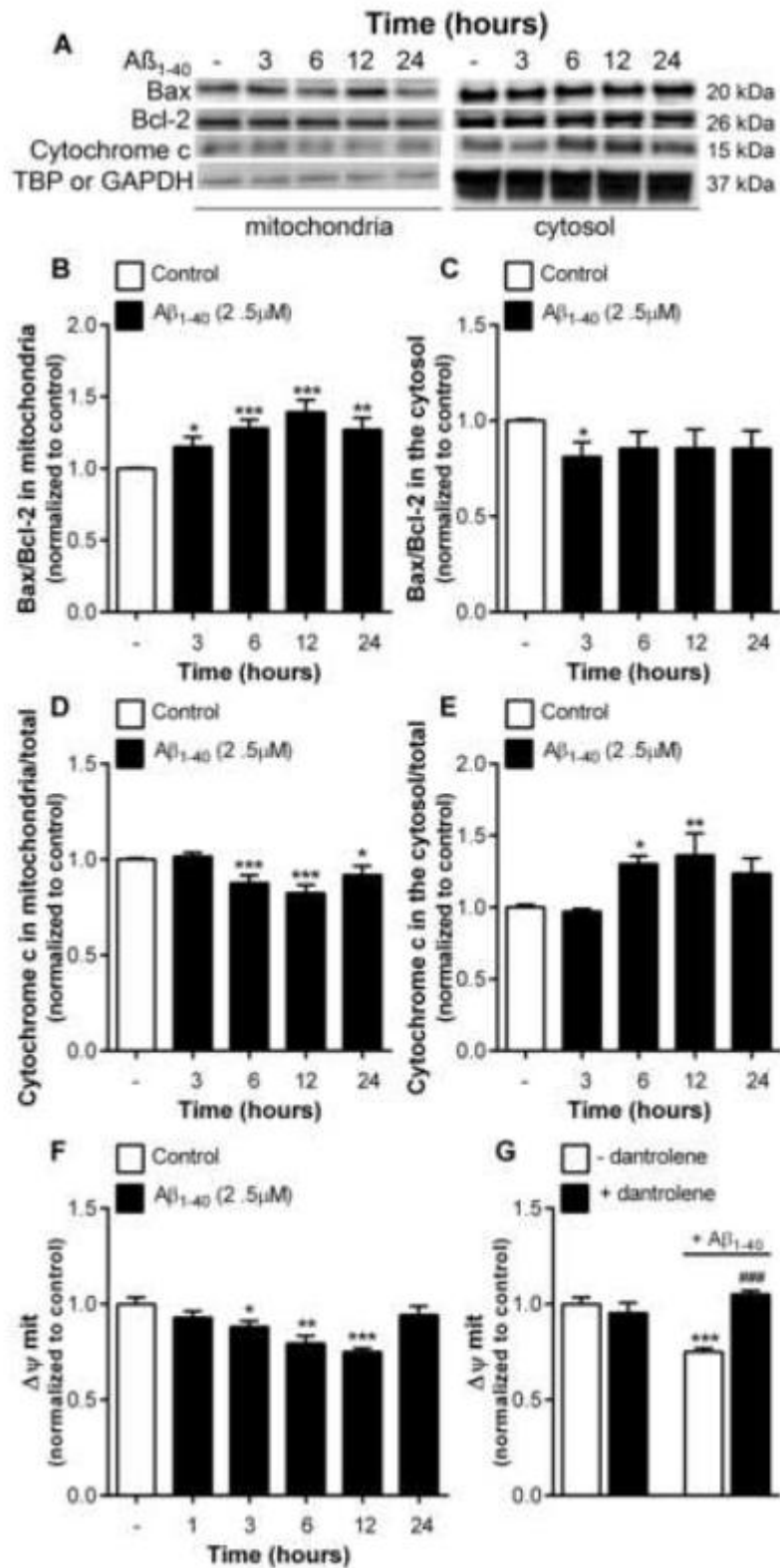


Figure 5

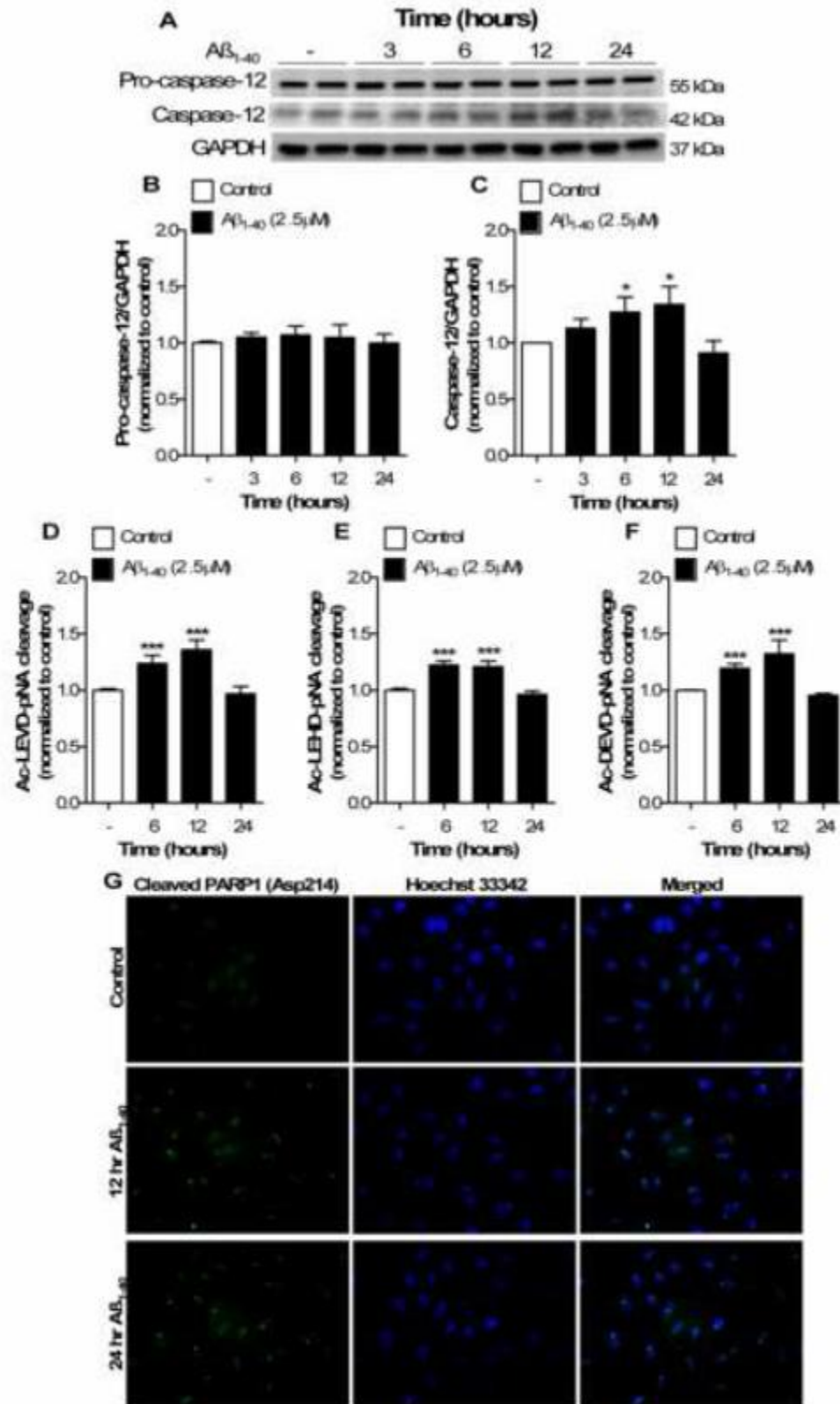


Figure 6

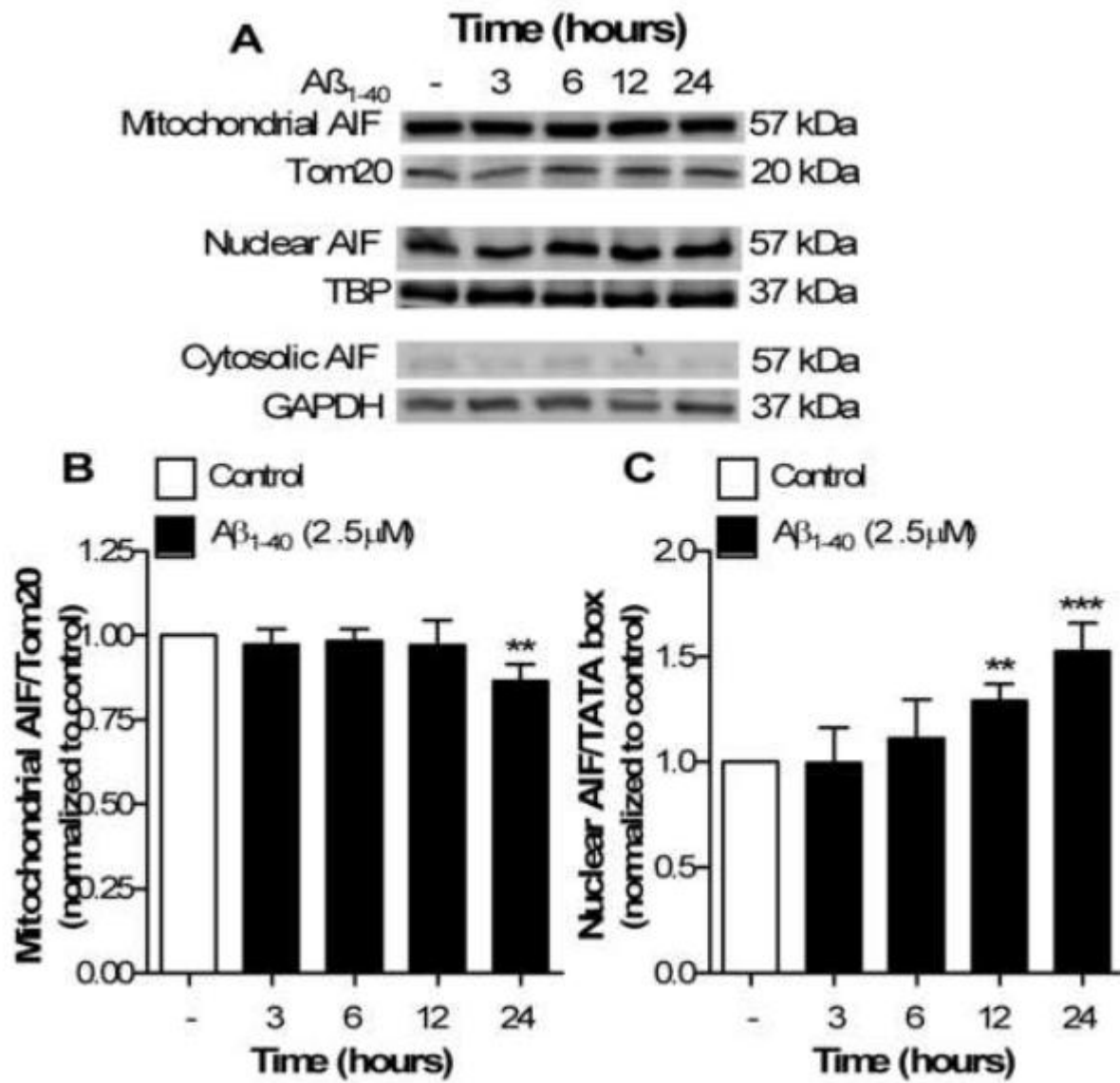


Figure 7

A

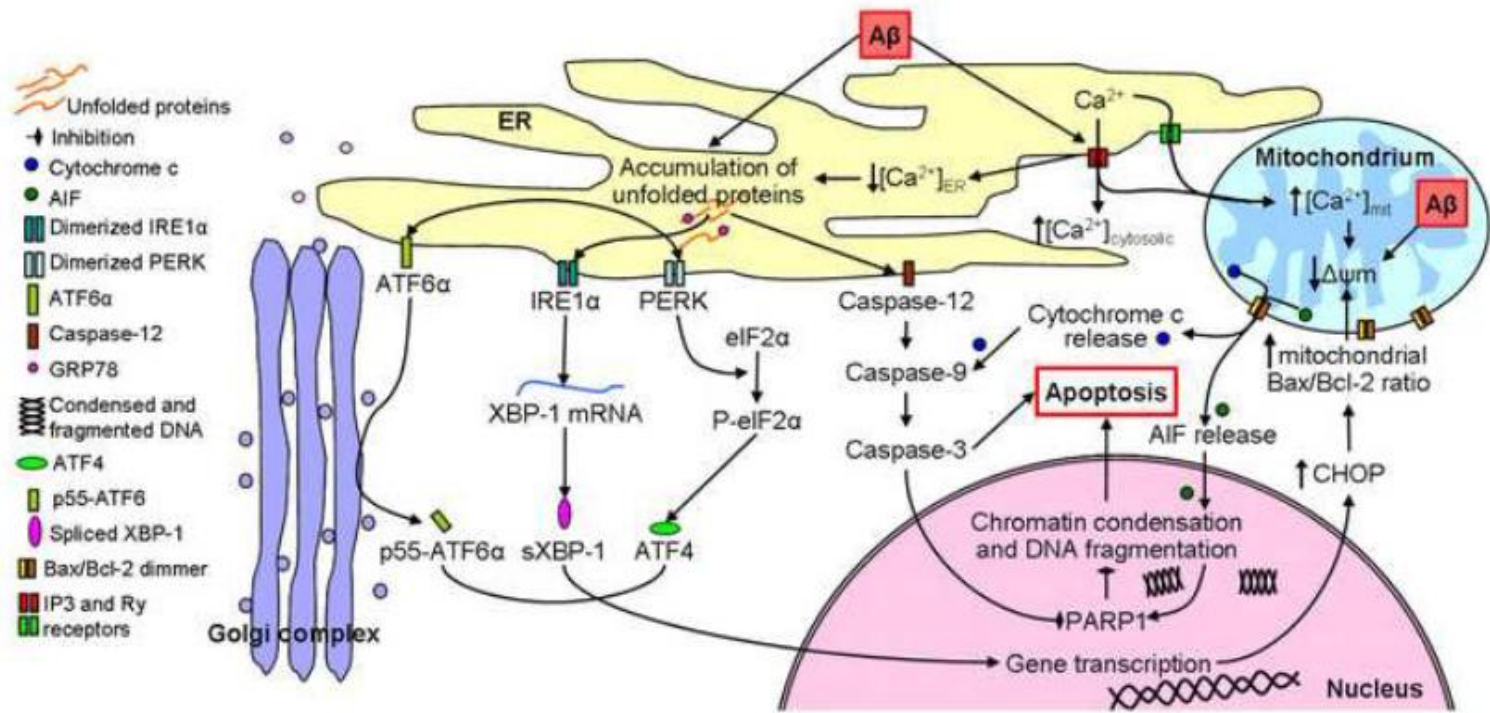


Figure 8

ACCEPTED

Highlights

The A β_{1-40} peptide in rat brain endothelial cell line (RBE4) induces:

- i) ER stress, increasing the levels of several mediators of UPR signalling pathways
- ii) loss of ER Ca²⁺ homeostasis concomitantly increasing cytosolic Ca²⁺ levels
- iii) upregulates the ER stress-associated pro-apoptotic transcription factor CHOP
- iv) activation of a mitochondria-independent cell death pathway through caspase-12
- v) caspase-dependent and independent apoptosis through cytochrome c and AIF

ACCEPTED MANUSCRIPT